Identification of Food-Derived Peptide Inhibitors of Soluble Epoxide Hydrolase

By

Joy Obeme-Nmom

A thesis submitted in partial fulfilment of the requirements

for the Master's degree

in Chemistry and Biomolecular Sciences

Department of Chemistry and Biomolecular Sciences

Faculty of Science

University of Ottawa

DEDICATION PAGE

This thesis is dedicated to God Almighty. To Him alone be all the glory.

TABLE OF CONTENTS

LIST OF FIGURES

LIST OF TABLES

ABSTRACT

Over the course of more than ten years, there has been a significant increase in the approach employed to inhibit the function of soluble epoxide hydrolase (sEH). The phenomenon of upregulating soluble epoxide hydrolase (sEH) has been found to result in a decrease in the ratio of epoxyeicosatrienoic acids (EETs) to dihydroeicosatrienoic acids (DHETs) in the body. This has garnered significant attention due to the diverse biological functions attributed to EETs, including the regulation of vasodilation, neuroprotection, increased fibrinolysis, calcium ion influx, and anti-inflammatory effects. Consequently, there has been a growing interest in developing and discovering sEH inhibitors through chemical syntheses and natural extracts, with the aim of increasing the availability of these anti-inflammatory molecules by reducing their hydrolysis. A comprehensive examination of this project was conducted to explore the inhibitory effects of YMSV, a tetrapeptide derived from the castor bean (*Ricinus communis*), on sEH, as well as to elucidate its underlying mechanism of action. YMSV was determined to function as a mixed-competitive inhibitor of soluble epoxide hydrolase (sEH), and the interaction between the peptide and the protein resulted in the disruption of the secondary structural composition of sEH. Furthermore, the hydrogen bond interactions between YMSV and the Asp 333 residue in the active region of soluble epoxide hydrolase (sEH) were demonstrated using molecular docking investigations. However, quantitative structure-activity relationship (QSAR) research revealed that nonpolar, hydrophobic, and bulky amino acids are favored at the N- and C- terminals of peptides for sEH inhibition. The results of this study indicate that peptides obtained from dietary sources possess unique characteristics as inhibitors of soluble epoxide hydrolase (sEH), displaying significant potency. Consequently, these peptides have promise for further development as therapeutic medicines targeting inflammation and depression in the future.

ACKNOWLEDGEMENTS

I would like to express my sincere appreciation to my supervisor, Prof. Chibuike Udenigwe, who bet on me and gave me a chance to explore my potential. Thank you for your patience, guidance, corrections, and encouragement, you have broadened my mind in the way I see research and life generally. I do not take your mentorship for granted.

Special thanks to my co-supervisor Prof. Paul Mayer as well as Prof. Apollinaire Tsopmo and Prof. Nicolas Bordenave for taking the time to sit on my Thesis Advisory Committee (TAC), contributing significantly by bringing their perspective to my research and reviewing my thesis.

I also acknowledge my parents, Arc. Chukwuma and Mrs. Ikeola Nmom for their love, prayers and support which kept me motivated throughout the program. To my siblings, Joanna, Juliana, James, and Juliet, you are the reason I work so hard.

To the absolute love of my life, Ifeanyi, you have been my pillar of support through this journey, thank you for everything. I can't fail to acknowledge my dear friends Josephine, Nifemi and Raliat. I am grateful for your kindness, guidance, feedback, friendship, and mentorship throughout this project. I love you all and your friendship means the world to me. Thank you for always being there for me.

Finally, this research was supported by the University of Ottawa Nutrition and Mental Health Scholarship, the Natural Sciences and Engineering Research Council of Canada (NSERC) Discovery Grant, and the University Research Chairs Program, University of Ottawa.

CHAPTER 1 – INTRODUCTION

1.1. Background of the study

Depression and mental health issues have become common phenomena and terms used in our world today and following the Covid-19 epidemic, research has predicted a worldwide surge in the incidence of major depressive disorder (Cénat et al., 2021; Santomauro et al., 2021). The World Health Organization (WHO) has reported that about 300 million people, which is approximately 3.8% of the world's population are undergoing depression, of which 5% are young adults and 5.7% are elderly people, with two times higher prevalence in women than men (WHO, 2019). Depression can also be experienced by young children as well as teenagers and these usually go undiagnosed (Li et al., 2022; Rieffe & De Rooij, 2012). Depression significantly impacts individuals and society, affecting cognitive and emotional functions, causing despair, loneliness, and worthlessness. It can lead to physical symptoms like sleep issues and sleep deprivation. Severe depression can increase the risk of self-harm and suicide (Zimmerman et al., 2018). Societal consequences include diminished production, healthcare costs, and increased reliance on social assistance systems. Treatment should focus on medical interventions rather than psychological approaches. Reducing depression's prevalence can be achieved through stigma reduction, public awareness, and accessible treatment options, fostering optimism, resilience, and adaptability (Kupferberg et al., 2016; Weightman et al., 2019).

While the common antidepressants are focused on neurotransmitter pathways activation and/or blockade, current literature shows that inflammation in the brain is highly associated with depression and the inflammatory pathway is a new therapeutic approach to the treatment and management of depressive symptoms (Borsini, 2021; Hashimoto, 2016). Interestingly, the arachidonic acid cascade has been reported to play a vital role in the inflammatory response of the body and contains anti-inflammatory metabolites known as epoxy fatty acid (EpFAs) which are rapidly degraded by the protein soluble epoxide hydrolase (sEH) to yield their less active 1,2- diols which have pro-inflammatory effects (Bellien & Joannides, 2013). However, the inhibition of sEH automatically restores the anti-inflammatory condition of the body due to the upregulation of EpFAs which decreases inflammatory cytokines and mediators (Rand et al., 2017). Consequently, several inhibitors of sEH have been discovered over the years with some going into clinical trials; however, poor pharmacokinetics and low oral bioavailability have limited the use of these

inhibitors as standard therapeutic applications for inflammation and by extension, depression(Shen & Hammock, 2012). In this chapter, the structure, function, and potential of known sEH inhibitors are discussed, with particular emphasis on the drawbacks and possibilities of their therapeutic use as anti-inflammatory medications and antidepressants.

1.2. Soluble Epoxide Hydrolase as a Therapeutic Target

Soluble epoxide hydrolase (sEH), initially termed cytosolic epoxide hydrolase (CEH), was originally identified in an insect developmental biology study and is predominantly found including humans and many other vertebrates (Hashimoto, 2019). sEH is a multifunctional enzyme with distinct N-terminal and C-terminal halves. It forms a 120 kD homodimer, encoded by the EPHX2 gene, and its hydrolase C-domain is responsible for hydrolyzing epoxides into diols, facilitating their excretion from cells (Morisseau & Hammock, 2005). Additionally, sEH plays a crucial role in the hydrolysis of lipid phosphates in its phosphatase N-domain, impacting cell proliferation (Kramer & Proschak, 2017). The sEH catalytic pocket comprises essential structural elements, including a catalytic triad involving Asp333, Asp495, and His523, which initiates the hydrolysis process. Hydrophobic residues, Tyr381 and Tyr465, assist in substrate binding and protection from solvent molecules. Variations in these residues affect substrate selection and catalytic efficiency among sEH isoforms (Arand et al., 2005; Gomez, 2006). The enzyme is present in numerous tissues, including the liver, heart, kidneys, intestines, and various brain regions, contributing to a wide range of physiological functions, such as immune response, blood vessel maintenance, and carcinogenesis (Gautheron & Jéru, 2021; Sun et al., 2021).

The primary substrates of sEH are epoxy fatty acids (EpFAs) which are metabolites of Polyunsaturated fatty acids (PUFAs), particularly those from arachidonic acid (ARA), as well as docosahexaenoic acid (DHA), and eicosapentaenoic acid (EPA) which are hydrolyzed into metabolites that are used for natural signaling in the body by the cytochrome P450 enzymes, cyclooxygenases (COXs) and lipoxygenases (LOXs) that produce epoxy and hydroxy eicosatetraenoic acids (EETs and HETEs), lipoxins and leukotrienes as well as prostaglandins respectively. In addition, these metabolites are known as oxylipins, and they are involved in the regulation and resolution of inflammatory pathways in tissues. sEH specifically catalyzes four isomers of EETs (5,6-, 8,9-, 11,12-, and 14,15-EETs) at the catalytic site of its C-terminal, these EET substrates are derived from the metabolism of arachidonic acids by cytochrome P450

enzymes; CYP2C and CYP2J. The product of the sEH metabolism of EETs is DHETs (dihydroxyeicosatrienoic acids) which are less active and easily excreted from the body (Wang et al., 2021). Apart from being degraded by sEH, EETs can also be metabolized through other biological pathways such as beta-oxidation, and fatty acid elongation, however, in rare cases, they can also go through COX, LOX and Cytochrome P450 w-oxidases (Imig et al., 2019).

EETs possess various beneficial biological activities, including vasodilation, anti-inflammatory effects, cardiovascular protection, neuroprotection, and antitumor effects. Notably, they influence vascular function by inducing endothelial and smooth muscle relaxation. A reduction in sEH expression can lead to increased EET levels, inhibiting sodium absorption, improving endothelial function, and reducing hypertension (Bellien & Joannides, 2013; Yang et al., 2015). Additionally, EETs exhibit anti-inflammatory properties by reducing the expression of inflammatory markers, inhibiting COX-2 overexpression, and promoting fibrinolysis (Capdevila et al., 2014; M. A. H. Khan et al., 2014). These characteristics make EETs promising candidates for managing metabolic disorders.

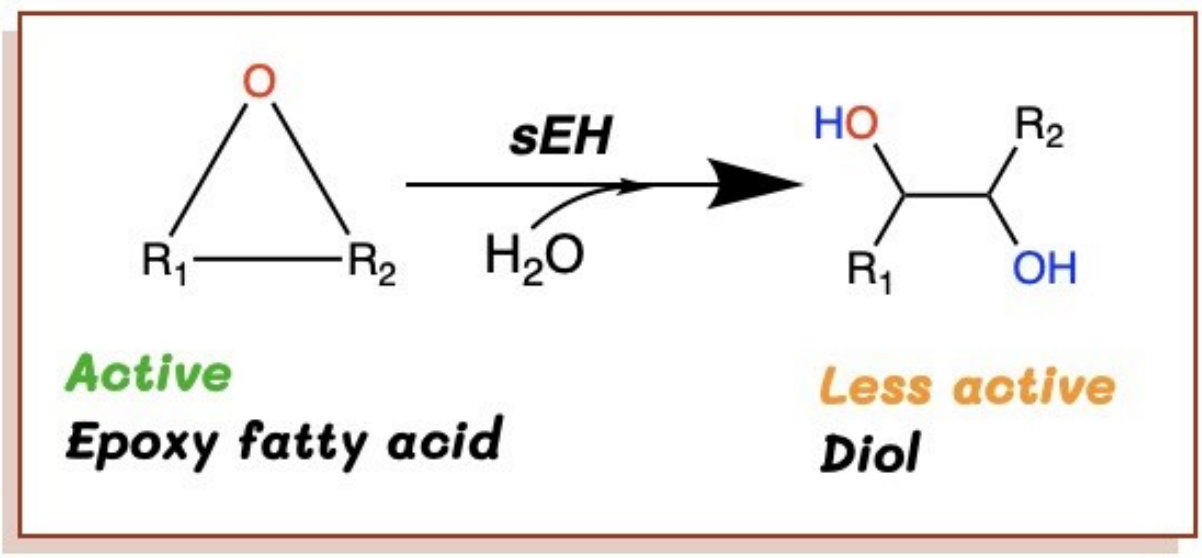

Figure 1.1. Reaction catalyzed by soluble epoxide hydrolase.

Table 1.1. Structures of EET isomers and their corresponding diols.

ENZYME	SUBSTRATE	PRODUCT
Soluble Epoxide Hydrolase (sEH)	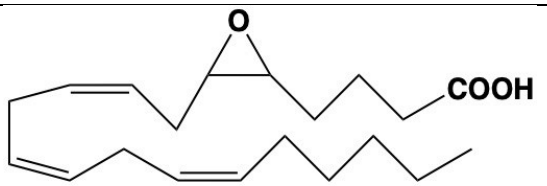 14,15-EET	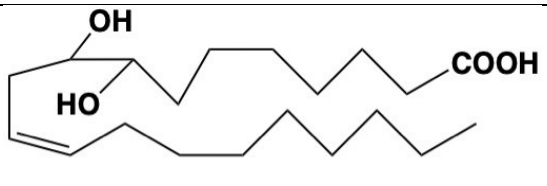 14,15-DHET
	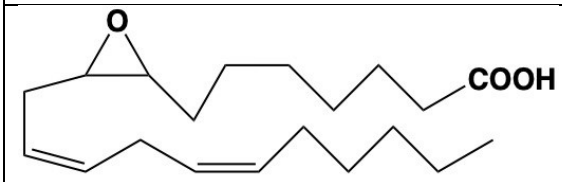 11,12-EET	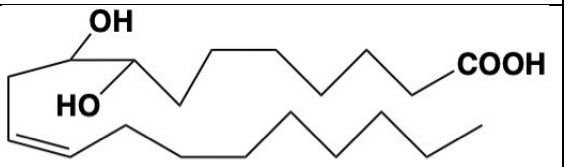 11,12-DHET
	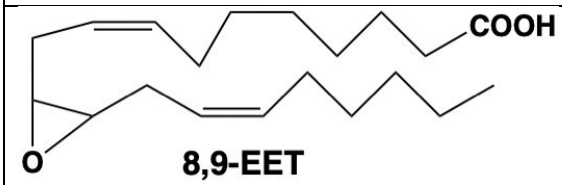 8,9-EET	 8,9-DHET
	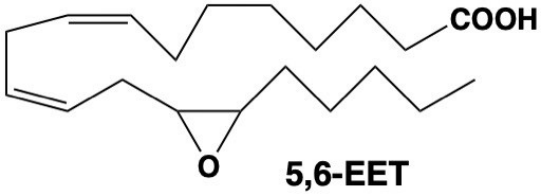 5,6-EET	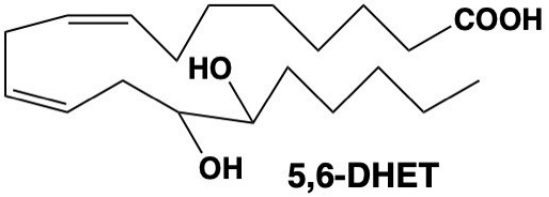 5,6-DHET

1.3. Soluble Epoxide Hydrolase Inhibitors

Understanding the structure of the enzyme's catalytic pocket has made it easier to find inhibitors of sEH. By exploiting the specific interactions and properties of the catalytic pocket, researchers have been able to design compounds that bind to the catalytic pocket and restrict sEH enzymatic activity. These inhibitors have been successfully used therapeutically in animal studies of cancer, inflammation, and hypertension (Iyer et al., 2022). The evolution of sEH inhibitors has been reported over the years and in the past decade, the central pharmacophores of these inhibitors have been amides, carbamates, heterocycles, and urea; with their IC_{50} in the micromolar to nanomolar range. In general, the amino group of the inhibitor serves as a hydrogen bond donor to the Asp333 residue while the carbonyl oxygen from the functional group of inhibitors establishes hydrogen bonds with the Tyrosine residues in the catalytic pocket; Try465 and Try381, generating a competitive inhibition. In addition, the functional groups of various inhibitors can also bind to the F265 and W334 binding pockets in the C-domain of the enzyme (Shen & Hammock, 2012). This section will discuss the common selective, dual, and natural sEH inhibitors, highlighting the developmental stages and applications as well as the shortcomings of these sEH inhibitors.

1.3.1 Selective sEH Inhibitors

The first compounds reported to inhibit sEH were chalcone oxides and glycidols. They were reported to demonstrate slow binding inhibition of the enzyme, forming a stabilized enzyme-inhibitor complex and were used to understand the active site of sEH. Preliminary studies by Dietze et. al (Dietze et al., 1991, 1993) demonstrated that the hydroxyl group plays a crucial role in the mechanism of glycidol inhibition. The study proposed a model for the interaction of 3-(4-nitrophenyl)glycidol with the active site of sEH, suggesting that glycidol enantiomers lacking a hydrogen bonding interaction should be classical competitive inhibitors and concluded that it should be possible to design an active site-directed irreversible inhibitor of sEH by placing an electrophile in the position occupied by the hydroxyl hydrogen of (2S,3S)-3-(4_nitrophenyl)glycidol (Dietze et al., 1991). In another study investigating the mechanism of chalcone oxide derivatives as sEH inhibitors, structural and kinetic evaluations, and testing on human and murine sEH were carried out. Recombinant mouse sEH (MsEH) and human sEH (HsEH) enzymes displayed optimum pH of 7.4 and 7.6 respectively. The K_ms for MsEH and HsEH

were 5.8 and 3.6 mM under these conditions, and the MsEH kcat was twofold higher than that of HsEH. Structure-activity relationship (SAR) studies of chalcone oxide derivatives identified optimal steric constraints and supported a mechanism of inhibition consistent with the electronic stabilization of an enzyme-inhibitor intermediate. (Morisseau et al., 1998). Both chalcone oxides and glycidols are potent selective inhibitors of sEH, with their inhibitory activity associated with hydrophilicity. Although chalcone oxides and glycidols have similar, yet distinct mechanisms of inhibition, trans-3-phenylglycidols were reported to be less potent than chalcone oxides. Unfortunately, these inhibitors showed poor stability and temporary effects on sEH *in vivo*, additionally, the quick hydrolysis of these compounds disqualified them from being drug candidates (Imig et al., 2019; Shen & Hammock, 2012).

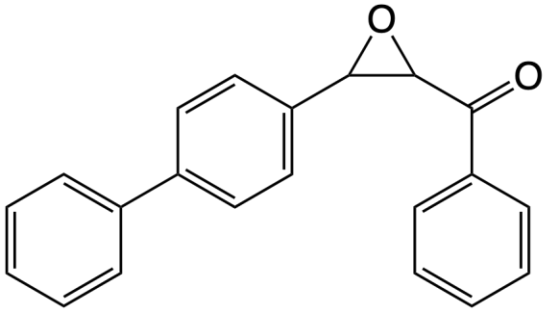

Chalcone oxide

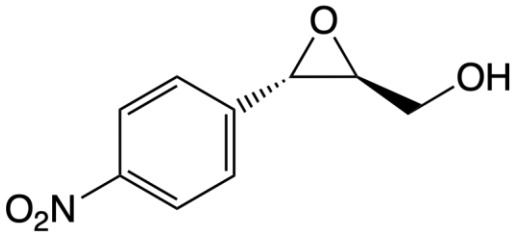

3-(4-Nitrophenyl)glycidol

The next class of inhibitors developed were highly stable and potent and constituted of urea, amide and carbamate derivatives. The first member of this new class is a urea derivative, DCU (N, N′-dicyclohexyl-urea) with a lower IC_{50} of 90nM and 160 nM for MsEH and HsEH respectively showing competitive and tight inhibition at the enzyme's active site (Morisseau et al., 1999). *In vivo* studies in hypertensive rats, DCU increase the ratio of EETs/DHETs by a significant 65% decrease in 14,15-DHET urinary excretion was observed in DCU-treated rats, along with a 30% increase in 14,15-EET urinary excretion, indicating *In vivo* DCU-mediated inhibition of sEH and showed vasoactive effects by decreasing blood pressure (Yu et al., 2000). DCU was later reported to have low water solubility and high melting point because of its inflexible structure and absence of a polar group which affected its oral absorption and bioavailability (Sun et al., 2021). Due to

the strong binding ability of urea inhibitors by strong hydrogen bond interactions and with the amino acid residues in the catalytic pocket, they were continuously developed with added modifications.

The DCU inhibitor was modified to produce AUDA (12-(3-adamantan-1-yl-ureido) dodecanoic acid) with improved water solubility and lower melting point. This was achieved by the introduction of carboxylic acid (a polar side chain) on one side of the urea backbone to increase the flexibility of the inhibitors (Morisseau et al., 2002). In a recent study, 25 mg/L of AUDA was continuously administered to Streptozotocin-induced type 1 diabetic (T1D) rats for 6 weeks in drinking water and treatment resulted in reduced oxidative stress and NADPH oxidase activity, suggesting that upregulating EETs derived from CYP2C11, inactivation of vascular endothelial growth factor A (VEGF-A) signaling pathway and inhibition of Nox4 expression attenuates diabetes-associated kidney malfunction (Njeim et al., 2023). AUDA also prevented cell proliferation and migration of human aorta smooth muscle cells by inhibiting TNF-induced proliferation and preventing cell death thereby showing the effect of sEH inhibition in atherosclerosis and other cardiovascular diseases (Li et al., 2017). Although AUDA is a competitive inhibitor of sEH and retained the inhibitory potency after modification, it had poor pharmacokinetic properties, including b-oxidation by cytochrome P450 enzymes resulting in its rapid metabolism and excretion in the biological system, which prevent it from being used for pharmacodynamic and clinical studies (Duflot et al., 2014).

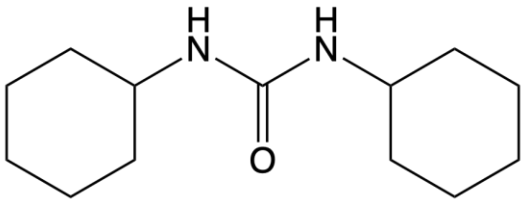

DCU

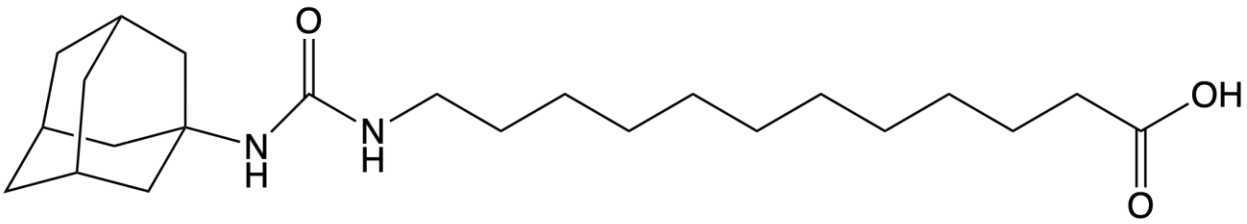

AUDA

Despite the addition of the polar group to the early 1,3-disubstituted urea inhibitors of sEH and the preserved potency of the inhibitor, the unsatisfactory pharmacokinetic properties like low water solubility and bioavailability created a need for more research to be done in order to design inhibitors with better physical and pharmacokinetic parameters with improved inhibitory potentials. The effectiveness of urea derivatives is due to their ability to mimic the transition state for epoxide ring opening, with their inhibitory properties revealed through crystal structures. Studies were carried out on the structure-activity relationship of inhibitors to include new polar groups and conformational constraints to the urea backbone. In this new class of inhibitors, the former linker which was an alkyl chain was replaced with saturated rings such as piperidine, cyclohexane or isoxazole or in some cases non-saturated rings to connect the central and secondary pharmacophores. The potency of these inhibitors was enhanced by lipophilic functional groups like adamantyl, biphenyl, or halogens, due to the L-shaped hydrophobic pocket of sEH, located at the secondary pharmacophore with about 7 Å from the carbonyl end of the urea helped to increase the physical and pharmacodynamic parameters of inhibitors. The addition of a tertiary pharmacophore, linked by alkyl or cyclic groups like aryl, cycloalkyl or cycloamino groups at about 17 Å from the carbonyl end of the urea greatly improved the water solubility of the inhibitors without affecting their potencies (Jones et al., 2006). Piperidine-based urea inhibitors APAU and TPAU have IC_{50} of 7 and 1.1 nM respectively, having an area under the curve (AUC) 10 times that of AUDA which contributed to better pharmacokinetics (Schäfer et al., 2015). The cyclohexane-based urea inhibitor AUCB was developed by Sung et. al, based on the skeleton of APAU, two isomers; *cis*-4-(4-(3-adamantan-1-yl-ureido) cyclohexyloxy) benzoic acid (*c*-AUCB) and *trans*-4-(4-(3-adamantan-1-yl-ureido) cyclohexyloxy) benzoic acid (*t*-AUCB) were created because of their closeness in structure. Similarly, half maximal inhibitory concentrations (IC50) of 1.3 and 0.89 μM were observed for *t*-AUCB and *c*-AUCB respectively with the former being more metabolically stable in human liver microsomal cells, having an AUC 40 times that of AUDA in dogs showing increased bioavailability of cyclohexane-based urea inhibitors (Tsai et al., 2010). The study also demonstrated that the newly inserted free carboxyl group creates a hydrogen connection with Met418 in addition to the urea function's hydrogen contacts with Asp333 and Tyr381 (Sung et al., 2007). *c*-AUCB has been applied in the treatment of Angiotensin II hypertensive ren-2 transgenic rats (TGR). Treatment with 26 mg/L inhibitor for 48 h reduced the blood pressure (BP) of TGR by reduction of Angiotensin II (Ang II) levels in the blood and

subsequently increasing the endogenous EET level (Varcabova et al., 2013). In a model of chronic kidney disease linked with hypertension induced by Ang II, administration of 3 mg/L of *c*-AUCB to the drinking water of TGRs exposed to 5/6 renal mass reduction (5/6 NX) after 20 weeks not only showed antihypertensive activity by reducing BP as reported earlier but also increased the survival rate from 25 to 72 %, preserved renal function by preventing a decrease in creatine clearance, decreased glomerulosclerosis and glomerular volume by regulating hydrolysis of EETs in the kidney (Kujal et al., 2014). Similarly, *t*-AUCB upregulated AMPK/Akt/eNOS signaling, repairing endothelial relaxation of the external maxillary artery, and preventing dysfunction of salivary glands in hypertensive rats (Han et al., 2022). Moreover, *t*-AUCB reduces microvascular inflammation in the hippocampus of the brain and prevents cognitive decline by downregulating the differentially expressed genes (DEGs) upregulated in high-glycemic diet mice, thereby protecting against Alzheimer's disease (Nuthikattu et al., 2021).

Aromatic and aliphatic counterparts of adamantyl-urea inhibitors were designed to address their low drug concentration and short half-life, with improved metrics of inhibition and up to 5000 times more AUC than APAU, TPPU was developed (Lee et al., 2014). TPPU ((1-trifluoromethoxyphenyl-3-(1-propionylpiperidin-4-yl) urea) is a transition state enzyme inhibitor of sEH and is a well-established and commercially available inhibitor which has been used in studies of pain, and inflammation, cardiovascular diseases, and hypertension. A recent study by Abdalla et al. demonstrated the dose-dependent effect of TPPU in local therapeutic treatment of formalin-induced hyperalgesia in the temporomandibular joint (TMJ) of rats by significantly reducing the production of inflammatory cytokines IL-6, IL-1β, IL-12, MCP-1 and TNF-α, inflammatory mediators PGE2, LTB4, and CXCL1, and increasing levels of IL-10 which is vital in the endogenous regulation of inflammation. Histological analysis in the study showed that pretreatment with TPPU avoided mast cell degranulation and leukocyte infiltration which preserved the inflammatory status of the cells in the treated TMJ, thereby amplifying the analgesic and anti-inflammatory effect of sEH inhibition (Abdalla et al., 2022). It has been found that TPPU alleviates the activation of P2x7/Cathepsin/Fractalkine pathway in microglia cells of arthritis models, depresses the MAPK/NFkB pathway in pulmonary macrophages to protect against injury in the lungs (Basting et al., 2023; Zhang et al., 2023).

Another approach to developing sEH inhibitors considered that the endogenous substrates of sEH are stereoisomers and their metabolism also yielded stereoisomeric products, therefore researchers employed stereo configurations and stereoselectivity employed in their quest for more stable and potent inhibitors and discovered that different enantiomers of inhibitors can selectively inhibit sEH with different pharmacokinetic properties (Lukin et al., 2018; Manickam et al., 2016). Consequently, the undesirable pharmacokinetic parameters such as poor stability, solubility, permeability and retention time of urea inhibitors, a series of amide sEH inhibitors were designed by the modification of adamantyl-based urea inhibitors to retain one of its NH groups (Pecic et al., 2018; Rezaee et al., 2021).

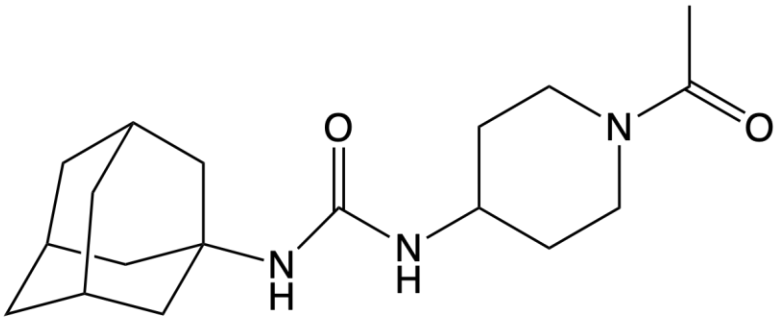

APAU

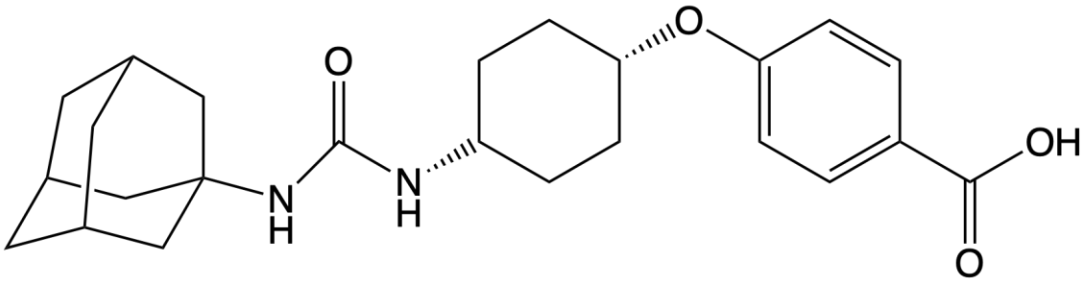

c-AUCB

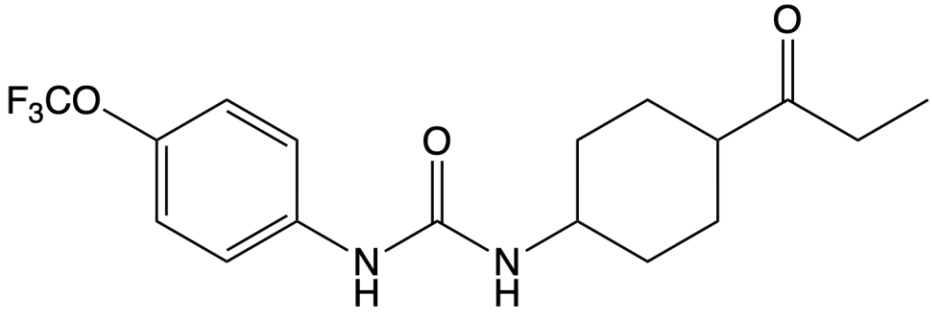

TPPU

1.3.2 Dual Inhibitors

Dual inhibitors are chemicals that block activity at two different enzymes or receptors. Compounds that inhibit sEH and have a secondary mechanism of action or target another enzyme or receptor may be referred to as "dual inhibitors" in the context of sEH inhibitors. The arachidonic acid metabolism plays a key role in the overall inflammatory response of the body and is a major target for inflammation and pain management. Therefore, the combination of the inhibition of sEH and that of other enzyme members of the arachidonic acid cascade has been explored for a synergistic anti-inflammatory effect in the treatment of numerous complex diseases (Hiesinger et al., 2019). Several drugs have been successfully found that regulate the cyclooxygenase and lipoxygenase components of the arachidonic acid metabolic pathway. Many NSAIDs (nonsteroidal anti-inflammatory drugs), for instance, block the enzymes cyclooxygenase-1 (COX-1) and cyclooxygenase-2 (COX-2). However, most NSAIDs are reported to have severe side effects such as stomach ulcers, headaches, and nausea, this informed the search for newer anti-inflammatory drugs with little or no side effects (Maniar et al., 2018). The rationale for the development of sEH dual inhibitors is simply to minimize proinflammatory mediators or molecules and elevate the level of anti-inflammatory molecules (Mahapatra et al., 2020).

PTUPB was designed as a dual inhibitor of sEH/COX-2 based on the skeleton of celecoxib; a selective COX-2 inhibitor, and *t*-AUCB a urea inhibitor of sEH. With an IC_{50} of 0.9 and 1.3 mM for sEH and COX-2 respectively, this compound was able to inhibit both enzymes while maintaining enough selectivity by forming hydrogen bonds with the catalytic triad of sEH as well as His90 and Tyr335 amino acid residues of COX-2 in mice (Maniar et al., 2018). Tumor development produced by hepatocellular carcinoma (HCC) was discovered to be suppressed by PTUPB via the downregulation of ER stress genes, resolution of the eicosanoid/cytokine storm, and stimulation of macrophage cleanup of debris (Fishbein et al., 2020). PTUPB was also found to be beneficial in the treatment of nonalcoholic fatty liver disease (NAFLD) through inhibition of the PI3K/AKT/mTOR/ Sirt1 pathway and diminishing of hepatocyte senescence (Zhang et al., 2022). Asides from PTUPB enhanced anti-inflammatory action and significantly lowered cardiovascular risks have been recorded for new urea-diarylpyrazole hybrids due to their simultaneous sEH/COX-2 inhibition (Abdelazeem et al., 2020). Leukotrienes (LTs) are proinflammatory lipid mediators which are generated through the 5-LOX pathway and several inhibitors for sEH, and 5-LOX have been developed over the years and have been reported to have

anti-inflammatory and endothelial cell adhesion properties (Hiesinger et al., 2019). More recently, an indoline-based compound was identified to act as a sEH/5-LOX inhibitor with IC_{50} of 0.41 and 0.1 mM respectively. *In vivo* studies demonstrated the anti-inflammatory efficacy of the compound in a zymosan-induced asthma rat model (Cerqua et al., 2022) The 5-LOX-activating protein (FLAP) plays a vital role in the formation of LTs by transferring free arachidonic acid molecules into the 5-LOX pathway, thereby making it a great anti-inflammatory target. Diflapolin was designed as the first sEH/FLAP inhibitor with very high specificity for both enzymes and showed anti-inflammatory activity in a zymosan-induced peritonitis mouse model by blocking leukocyte adhesion reduced LT C4 and B4 levels as well as suppressed vascular permeability (Garscha et al., 2017). Some dual sEH inhibitors target enzymes and receptors that are nonmembers of arachidonic acid cascade. For example, the dual inhibitors of sEH and FAAH (fatty acid amide hydrolase) have been used in the treatment of inflammation and neuropathic pain (Sasso et al., 2015). TPPPC was developed by Kodani et al. by a combination of TPPU and PF-3845, a poor sEH/FAAH inhibitor, and has nanomolar potencies (sEH IC_{50} = 5 nM, FAAH IC_{50} = 8 nM) with distinct selectivity for both enzymes (Kodani, Wan, et al., 2018).

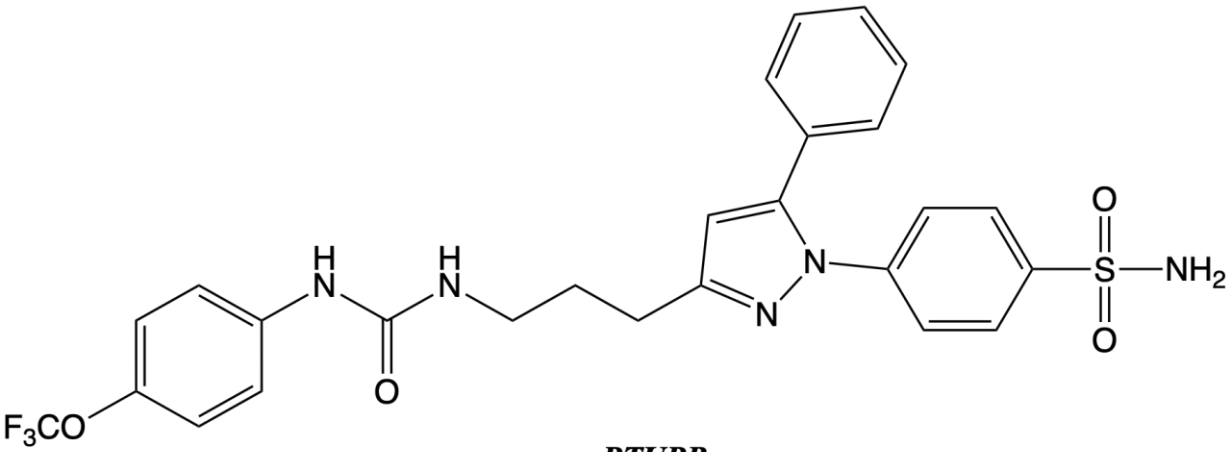

PTUPB

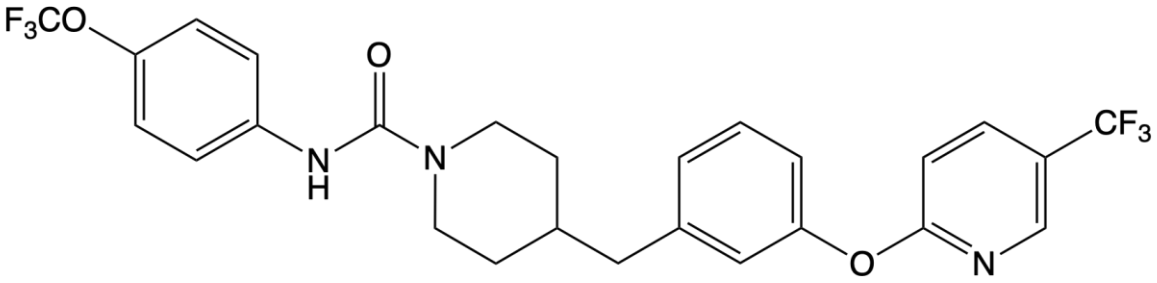

TPPPC

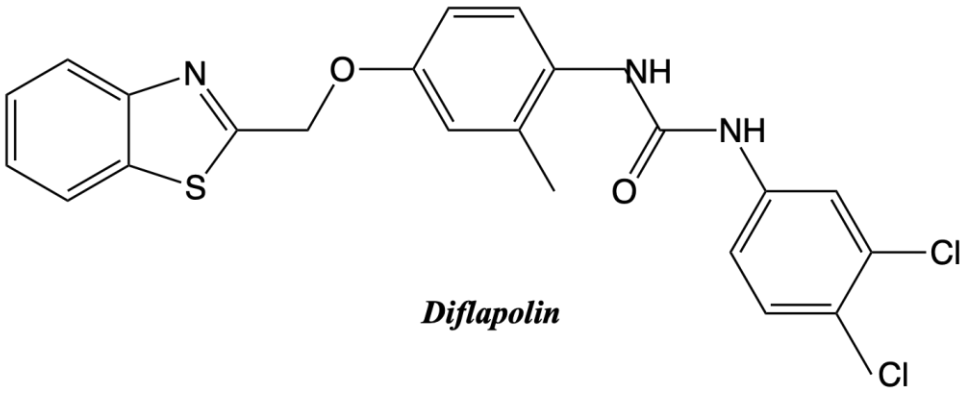

Diflapolin

1.3.3. Clinically Tested sEH Inhibitors

Soluble epoxide hydrolase inhibitors (sEHIs) are a family of drugs that have shown promise in a variety of preclinical investigations as well as certain early-stage clinical trials for the treatment of a variety of disorders. Such conditions include hypertension, inflammation, and cardiovascular diseases. Currently, there are three common inhibitors of sEH that have been clinically tested. Arete Therapeutics initially designed an sEH inhibitor AR9281 which improved endothelial function in animal models of hypertension and dysglycemia and was able to decrease the activity of sEH by up to 90%, thereby diminishing the level of dihydroxy fatty acids in healthy participants of a clinical study. Unfortunately, AR9281 was unable to go into phase II of the clinical trial despite its high selectivity and potency for sEH as well as its good pharmacokinetic properties (Anandan et al., 2011). The next inhibitor GSK2256294 was shown to have better pharmacokinetic profiles and drug-like qualities by combining simple cycloalkyl groups with conformationally constrained substituents. This compound underwent two phases I clinical trials in healthy non-smoker subjects and in overweight smokers, results showed that sEH was inhibited up to 41.9% and 99.8% with doses of 2 mg and 20 mg of the drug respectively and could be sustained in the plasma for up to a day. Although sEH inhibition by this compound was very rapid and highly sustained, it was slowly metabolized and excreted out of the body which is a bad PK characteristic, however, no serious adverse effect was noted in the subjects (Lazaar et al., 2016). More recently, the compound EC5026 by EicOsis Pharmaceuticals was selected for Phase 1a clinical trial due to its potency, moderate *in vivo* half-life, and ease of formulation. EC5026 is a slow-tight binding transition state mimic that inhibits the soluble epoxide hydrolase (sEH) at picomolar concentrations and is an oral drug designed for the treatment of neuropathic pain. The study concluded that when administered as a single oral dosage ranging from 0.5 to 24 mg, EC5026 is safe to use and well tolerated by patients and can be administered once per day. However, EC5026 was classified as a BCS Class 2 compound (high permeability and poor solubility), which limited formulation choices (Hammock et al., 2021). It is recommended that long-term studies should be conducted for these inhibitors in order to ensure their safety and stability.

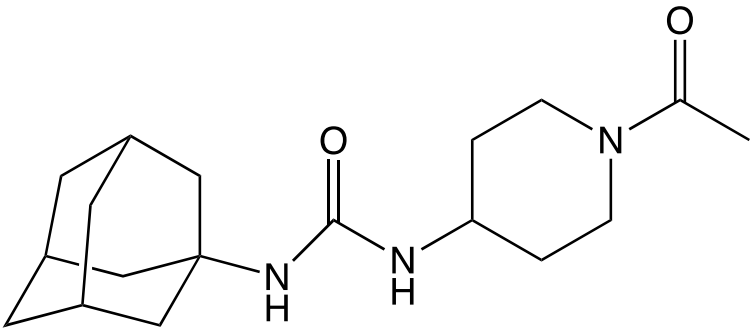

AR9281

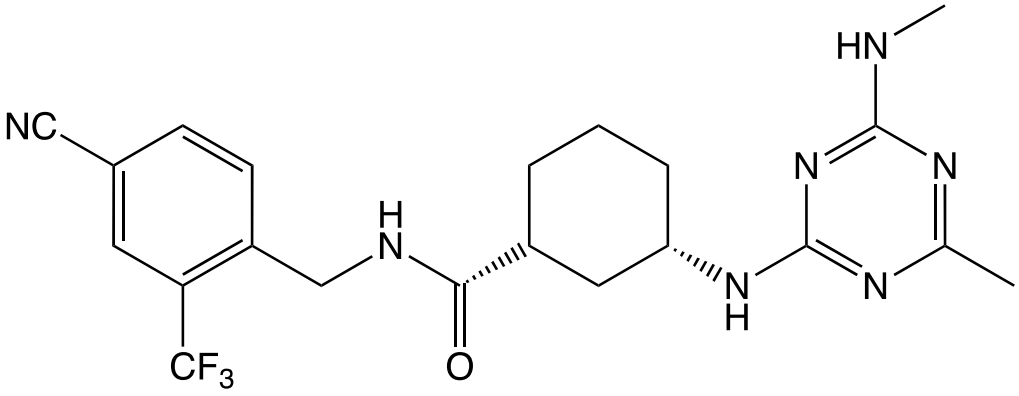

GSK225694

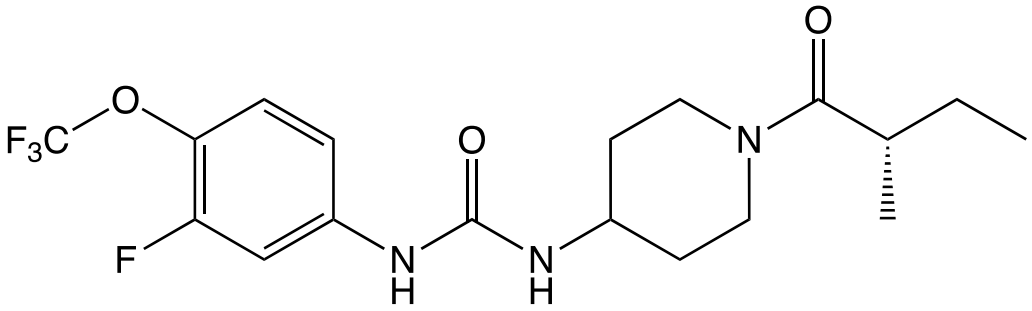

EC5026

1.4. sEH and Depression

Several lines of evidence have recently suggested that sEH distribution is critical in the development of inflammatory and brain disorders. Although there are no known specific biomarkers of depression, inflammation has been implicated in its physiopathology (Hennebelle et al., 2017). The levels of various biomarkers of inflammation such as tumor necrosis factor (TNF), interleukin-1, interleukin-6, acute-phase protein C-reactive protein (CRP), and proinflammatory cytokines have been established to be increased in the blood of patients with major depressive disorders (Lotrich et al., 2011). Some schools of thought believe that inflammatory biomarkers associated with depressive symptoms may be brought about by pre-existing medical conditions such as cancer, cardiovascular diseases, and neurodegenerative diseases (Swardfager et al., 2018).

The hydrolysis of epoxyeicosatrienoic acids, EETs by sEH into their corresponding less bioactive dihydro-eicosatrienoic acids (DHETs) reduce the overall response to inflammation in the body because these EETs have been shown to mediate vasodilatation, reduce inflammation, attenuate oxidative stress, and block the pathological endoplasmic reticulum (ER) stress response (Griñán-Ferré et al., 2020). The role of the EpFA in regulating inflammatory conditions, particularly in the brain is a potential target and inhibiting sEH as a strategy to sustain their biological activity is a novel approach with great promise (Wagner et al., 2017). Upregulation of EETs by treatment with EET analogs has been reported to attenuate cisplatin-induced renal oxidative stress, inflammation, and ER stress. EET analogs reduced the renal expression of all inflammatory marker genes by 40 –75%, elevated TNF-αlevel by 65–70%, markedly increased renal SOD expression, and reduced kidney MDA levels to values similar to WKY rats, EETs up-regulate the expression and activity of SOD during toxic insult and consequently enhance ROS scavenging and oxidative stress reduction (Khan et al., 2013).

In a study by (Wu et al., 2017), the deletion of the sEH gene (Ephx2) also significantly reduced the expression of proinflammatory mediators IL-1β, IL-6, MIP-2, and MCP-1 and resulted in an elevation of EET levels and the EET/DHET ratio in mice after induction with Intracerebral hemorrhage (ICH). Levels of proinflammatory cytokines IL-1β, IL-6, and MIP-2 were significantly attenuated following pharmacological inhibition by AUDA, a selective sEH inhibitor, in hemorrhagic brains compared with the vehicle group at 1-day post-ICH. However, *in vitro*

determination of the effects of gene deletion and inhibition of sEH on neuroinflammation in BV2 microglial and primary microglial cells ultimately reduced NO production indicating a reduction in oxidative stress. Their results suggest that AUDA inhibits thrombin- and hemin-induced microglial activation and limits the production of inflammatory mediators by suppressing the P38 MAPK and NF-κB pathways. Additionally, the sEH gene promoter region contains recognition sites for specificity protein (SP)-1, a transcription factor that responds to inflammatory signals and oxidative stress (Zhang et al., 2010).

Taken together, we can infer that inflammation and oxidative stress could be part of the mechanisms used by the enzyme sEH to cause depression and inhibition of the enzyme play a protective role in major organs in the human body.

1.5. Food-derived peptides

Food-derived peptides have not just been studied for their nutritional properties and functions but also for their biological roles and how easily they can be located by tissues and cells where they are needed in the body. Some of the biological roles that have been identified include antimicrobial, anti-inflammatory, antidiabetic, and antihypertensive. The anti-inflammatory properties of food-derived bioactive peptides, as well as their potential to be used for treatment, prevention, or management of life-threatening illnesses such as cardiovascular diseases (Gu & Wu, 2016), inflammatory bowel disease (Daskalaki et al., 2021; Fernández-Tomé et al., 2019; H. Zhang et al., 2015), type2-diabetes, obesity, and osteoarthritis (McMasters et al., 2017) through potential inhibition of inflammation pathways, have been well established. Even though some of these peptides have been studied *in vitro*, through animal research, cell culture, and even clinical trials, commercial manufacturing of these food-derived bioactive peptides has lagged, and one reason for this is the overall lack of knowledge regarding gastrointestinal stability or absorption of these peptides, as well as the lack of knowledge regarding their mechanisms of action (Chakrabarti et al., 2015). Comparatively to larger or longer peptides, food-derived peptides with two to five amino acids chain length are anticipated to have significant prospects for translation as active ingredients of functional foods, and they have been projected to have more chances of being more biologically accessible to the brain. Due to their smaller number of scissile bonds and the ability to be carried through the intestine and into the blood by certain transporters, they are typically more resistant to gut proteolytic inactivation (Udenigwe et al., 2021). It has been reported that a

peptide, GPETAFLR could also reduce inflammation and confer protection to brain cells (Lemus-Conejo et al., 2022). This further supports the opinion that small food peptides may cross the blood-brain barrier or act through other tissues to exert important neurophysiological impact.

1.6. Conclusion

Several types of sEH inhibitors have been designed and established to be great candidates in the development of anti-inflammatory drugs for various cardiovascular, metabolic, and central nervous system (CNS) diseases. Most of the inhibitors employ hydrogen bonding and hydrophobic interactions when binding to the catalytic pocket of the enzyme. Although some of these inhibitors have high inhibitory potencies for sEH, most of them have poor pharmacokinetic properties such as low water solubility, LogP, high melting point and short retention time *in vivo,* creating a demand for the identification of newer inhibitors with more satisfactory parameters suitable for pharmacodynamic studies. Most studies on sEH inhibition have been geared toward the treatment and management of hypertension, however, inflammation has also been implicated in depression. Therefore, there is a need for more studies on the role of sEH as a therapeutic target for depression. Moreover, urea inhibitors of sEH have been classified as the most potent as well as their amide derivatives, thus suggesting that the amino group of peptides could be potential inhibitors of sEH as they possess similar functional groups. Plant-based protein hydrolysates have been chosen for this study because of the recorded health benefits of bioactive peptides which include antioxidant, anti-inflammatory, immunomodulatory, and possibly anti-depressant, and neuroprotection properties. Thus, it is worth investigating how these properties contribute to the mechanism of sEH inhibition.

1.6. Study Hypothesis and Objectives

1.6.1. Hypothesis

The presence of several dietary peptides has been reported in different tissues, including the liver and the brain. However, there is limited knowledge of the interaction of the food peptides and targets of major depressive disorder. The best inhibitors reported for sEH consist of the urea backbone and interestingly, amino acids have functional groups with similar structure.

Therefore, the hypothesis of this study is that food-derived peptides will inhibit human sEH activity *in vitro* due to their plethora of amide groups pharmacophore which are similar to the structure of classic urea inhibitors of the enzyme and consequently exhibit anti-inflammatory and

antioxidant properties in brain cells by increasing the EETs:DHETs ratio, potentially controlling depressive-like processes of the brain.

1.6.2. Objectives

The aim of the study is to identify food-derived peptides as potent, safe, and novel inhibitors of soluble epoxide hydrolase and investigate if the peptide bioactivities attenuate an indicator of the depressive state. **The specific objectives of this project** include; **a)** *in vitro* screening of food-derived peptides with other known biological activities for inhibitory sEH activity **b)** Evaluation of effects of identified peptides on sEH structure and activity via secondary structure analysis and molecular dynamic simulations **c)** Identification of the relationship between the structure and activity of the amino acid constituents of the food-derived peptides via quantitative structure-activity relationship (QSAR) modeling.

1.7. References

Abdalla, H. B., Napimoga, M. H., Teixeira, J. M., Trindade-da-Silva, C. A., Pieroni, V. L., dos Santos Araújo, F. S. M., Hammock, B. D., & Clemente-Napimoga, J. T. (2022). Soluble epoxide hydrolase inhibition avoid formalin-induced inflammatory hyperalgesia in the temporomandibular joint. *Inflammopharmacology*, *30*(3), 981–990. https://doi.org/10.1007/s10787-022-00965-5

Abdelazeem, A. H., Safi El-Din, A. G., Abdel-Fattah, M. M., Amin, N. H., El-Moghazy, S. M., & El-Saadi, M. T. (2020). Discovery of novel urea-diarylpyrazole hybrids as dual COX-2/sEH inhibitors with improved anti-inflammatory activity and highly reduced cardiovascular risks. *European Journal of Medicinal Chemistry*, *205*. https://doi.org/10.1016/j.ejmech.2020.112662

Anandan, S. K., Webb, H. K., Chen, D., Wang, Y. X., Aavula, B. R., Cases, S., Cheng, Y., Do, Z. N., Mehra, U., Tran, V., Vincelette, J., Waszczuk, J., White, K., Wong, K. R., Zhang, L. N., Jones, P. D., Hammock, B. D., Patel, D. V., Whitcomb, R., … Gless, R. (2011). 1-(1-Acetyl-piperidin-4-yl)-3-adamantan-1-yl-urea (AR9281) as a potent, selective, and orally available soluble epoxide hydrolase inhibitor with efficacy in rodent models of hypertension and dysglycemia. *Bioorganic and Medicinal Chemistry Letters*, *21*(3). https://doi.org/10.1016/j.bmcl.2010.12.042

Arand, M., Cronin, A., Adamska, M., & Oesch, F. (2005). Epoxide hydrolases: Structure, function, mechanism, and assay. In *Methods in Enzymology* (Vol. 400). https://doi.org/10.1016/S0076-6879(05)00032-7

Bellien, J., & Joannides, R. (2013). Epoxyeicosatrienoic acid pathway in human health and diseases. *Journal of Cardiovascular Pharmacology*, *61*(3). https://doi.org/10.1097/FJC.0b013e318273b007

Borsini, A. (2021). The role of soluble epoxide hydrolase and its inhibitors in depression. In *Brain, Behavior, and Immunity - Health* (Vol. 16). https://doi.org/10.1016/j.bbih.2021.100325

Capdevila, J. H., Pidkovka, N., Mei, S., Gong, Y., Falck, J. R., Imig, J. D., Harris, R. C., & Wang, W. (2014). The Cyp2c44 epoxygenase regulates epithelial sodium channel activity and the blood pressure responses to increased dietary salt. *Journal of Biological Chemistry*, *289*(7). https://doi.org/10.1074/jbc.M113.508416

Cénat, J. M., Blais-Rochette, C., Kokou-Kpolou, C. K., Noorishad, P. G., Mukunzi, J. N., McIntee, S. E., Dalexis, R. D., Goulet, M. A., & Labelle, R. P. (2021). Prevalence of symptoms of depression, anxiety, insomnia, posttraumatic stress disorder, and psychological distress among populations affected by the COVID-19 pandemic: A systematic review and meta-analysis. In *Psychiatry Research* (Vol. 295). https://doi.org/10.1016/j.psychres.2020.113599

Cerqua, I., Musella, S., Peltner, L. K., D'Avino, D., Di Sarno, V., Granato, E., Vestuto, V., Di Matteo, R., Pace, S., Ciaglia, T., Bilancia, R., Smaldone, G., Di Matteo, F., Di Micco, S., Bifulco, G., Pepe, G., Basilicata, M. G., Rodriquez, M., Gomez-Monterrey, I. M., Bertamino, A. (2022). Discovery and Optimization of Indoline-Based Compounds as Dual 5-LOX/sEH Inhibitors: In Vitro and in Vivo Anti-Inflammatory Characterization. *Journal of Medicinal Chemistry*, *65*(21). https://doi.org/10.1021/acs.jmedchem.2c00817

Chakrabarti, S., Guha, S., & Majumder, K. (n.d.). *Food-Derived Bioactive Peptides in Human Health: Challenges and Opportunities*. https://doi.org/10.3390/nu10111738

Daskalaki, M. G., Axarlis, K., Aspevik, T., Orfanakis, M., Kolliniati, O., Lapi, I., Tzardi, M., Dermitzaki, E., Venihaki, M., Kousoulaki, K., & Tsatsanis, C. (2021). Fish sidestream-derived protein hydrolysates suppress dss-induced colitis by modulating intestinal inflammation in mice. *Marine Drugs*, *19*(6). https://doi.org/10.3390/md19060312

Dietze, E. C., Kuwano, E., Casas, J., & Hammock, B. D. (1991). Inhibition of cytosolic epoxide hydrolase by trans-3-phenylglycidols. *Biochemical Pharmacology*, *42*(6). https://doi.org/10.1016/0006-2952(91)90250-9

Dietze, E. C., Kuwano, E., & Hammock, B. D. (1993). The interaction of cytosolic epoxide hydrolase with chiral epoxides. *International Journal of Biochemistry*, *25*(1). https://doi.org/10.1016/0020-711X(93)90488-Z

Duflot, T., Roche, C., Lamoureux, F., Guerrot, D., & Bellien, J. (2014). Design and discovery of soluble epoxide hydrolase inhibitors for the treatment of cardiovascular diseases. In *Expert Opinion on Drug Discovery* (Vol. 9, Issue 3). https://doi.org/10.1517/17460441.2014.881354

Fernández-Tomé, S., Hernández-Ledesma, B., Chaparro, M., Indiano-Romacho, P., Bernardo, D., & Gisbert, J. P. (2019). Role of food proteins and bioactive peptides in inflammatory bowel

disease. In *Trends in Food Science and Technology* (Vol. 88). https://doi.org/10.1016/j.tifs.2019.03.017

Fishbein, A., Wang, W., Yang, H., Yang, J., Hallisey, V. M., Deng, J., Verheul, S. M. L., Hwang, S. H., Gartung, A., Wang, Y., Bielenberg, D. R., Huang, S., Kieran, M. W., Hammock, B. D., & Panigrahy, D. (2020). Resolution of eicosanoid/cytokine storm prevents carcinogen and inflammation-initiated hepatocellular cancer progression. *Proceedings of the National Academy of Sciences of the United States of America*, *117*(35). https://doi.org/10.1073/pnas.2007412117

Garscha, U., Romp, E., Pace, S., Rossi, A., Temml, V., Schuster, D., König, S., Gerstmeier, J., Liening, S., Werner, M., Atze, H., Wittmann, S., Weinigel, C., Rummler, S., Scriba, G. K., Sautebin, L., & Werz, O. (2017). Pharmacological profile and efficiency in vivo of diflapolin, the first dual inhibitor of 5-lipoxygenase-activating protein and soluble epoxide hydrolase. *Scientific Reports*, *7*(1). https://doi.org/10.1038/s41598-017-09795-w

Gautheron, J., & Jéru, I. (2021). The multifaceted role of epoxide hydrolases in human health and disease. In *International Journal of Molecular Sciences* (Vol. 22, Issue 1). https://doi.org/10.3390/ijms22010013

Gomez, G. A. (2006). Human soluble epoxide hydrolase: Structural basis of inhibition by 4-(3-cyclohexylureido)-carboxylic acids. *Protein Science*, *15*(1). https://doi.org/10.1110/ps.051720206

Griñán-Ferré, C., Codony, S., Pujol, E., Yang, J., Leiva, R., Escolano, C., Puigoriol-Illamola, D., Companys-Alemany, J., Corpas, R., Sanfeliu, C., Pérez, B., Loza, M. I., Brea, J., Morisseau, C., Hammock, B. D., Vázquez, S., Pallàs, M., & Galdeano, C. (2020). Pharmacological Inhibition of Soluble Epoxide Hydrolase as a New Therapy for Alzheimer's Disease. *Neurotherapeutics*, *17*(4), 1825–1835. https://doi.org/10.1007/s13311-020-00854-1

Gu, Y., & Wu, J. (2016). The potential of antioxidative and anti-inflammatory peptides in reducing the risk of cardiovascular diseases. In *Current Opinion in Food Science* (Vol. 8). https://doi.org/10.1016/j.cofs.2016.01.011

Hammock, B. D., McReynolds, C. B., Wagner, K., Buckpitt, A., Cortes-Puch, I., Croston, G., Lee, K. S. S., Yang, J., Schmidt, W. K., & Hwang, S. H. (2021). Movement to the Clinic of Soluble Epoxide Hydrolase Inhibitor EC5026 as an Analgesic for Neuropathic Pain and for Use as a Nonaddictive Opioid Alternative. *Journal of Medicinal Chemistry*, *64*(4). https://doi.org/10.1021/acs.jmedchem.0c01886

Han, W. wen, Wang, X. rui, He, Y. feng, Zhang, H. shu, Cong, X., Xiang, R. L., Wu, L. L., Yu, G. Y., Liu, L. mei, & Zhang, Y. (2022). Soluble epoxide hydrolase inhibitor, t-AUCB, improves salivary gland function by ameliorating endothelial injury. *Life Sciences*, *308*. https://doi.org/10.1016/j.lfs.2022.120942

Hashimoto, K. (2016). Soluble epoxide hydrolase: a new therapeutic target for depression. In *Expert Opinion on Therapeutic Targets* (Vol. 20, Issue 10). https://doi.org/10.1080/14728222.2016.1226284

Hashimoto, K. (2019). Role of soluble epoxide hydrolase in metabolism of PUFAs in psychiatric and neurological disorders. In *Frontiers in Pharmacology* (Vol. 9, Issue JAN). Frontiers Media S.A. https://doi.org/10.3389/fphar.2019.00036

Hennebelle, M., Otoki, Y., Yang, J., Hammock, B. D., Levitt, A. J., Taha, A. Y., & Swardfager, W. (2017). Altered soluble epoxide hydrolase-derived oxylipins in patients with seasonal major depression: An exploratory study. *Psychiatry Research*, *252*, 94–101. https://doi.org/10.1016/J.PSYCHRES.2017.02.056

Hiesinger, K., Wagner, K. M., Hammock, B. D., Proschak, E., & Hwang, S. H. (2019). Development of multitarget agents possessing soluble epoxide hydrolase inhibitory activity. In *Prostaglandins and Other Lipid Mediators* (Vol. 140). https://doi.org/10.1016/j.prostaglandins.2018.12.003

Imig, J. D., Roos, J., Zhang, G., Yang, G.-Y., G-y, Y., Jones, R. D., Liao, J., Tong, X., Xu, D., Sun, L., & Li, H. (2019). *Epoxy-Oxylipins and Soluble Epoxide Hydrolase Metabolic Pathway as Targets for NSAID-Induced Gastroenteropathy and Inflammation-Associated Carcinogenesis*. *10*. https://doi.org/10.3389/fphar.2019.00731

Iyer, M. R., Kundu, B., & Wood, C. M. (2022). Soluble epoxide hydrolase inhibitors: an overview and patent review from the last decade [Article]. *Expert Opinion on Therapeutic Patents*, *32*(6), 629–647. https://doi.org/10.1080/13543776.2022.2054329

Jones, P. D., Tsai, H. J., Do, Z. N., Morisseau, C., & Hammock, B. D. (2006). Synthesis and SAR of conformationally restricted inhibitors of soluble epoxide hydrolase. *Bioorganic and Medicinal Chemistry Letters*, *16*(19). https://doi.org/10.1016/j.bmcl.2006.07.009

Khan, H. A. Md., Liu, J., Kumar, G., Skapek, S. X., Falck, J. R., Imig, J. D., -Khan, A. H., Liu, J., Kumar, G., & Skapek, S. X. (2013). Novel orally active epoxyeicosatrienoic acid (EET) analogs attenuate cisplatin nephrotoxicity; Novel orally active epoxyeicosatrienoic acid (EET) analogs attenuate cisplatin nephrotoxicity. *The FASEB Journal • Research Communication*, *27*(8), 2946–2956. https://doi.org/10.1096/fj.12-218040

Khan, M. A. H., Pavlov, T. S., Christain, S. V., Neckář, J., Staruschenko, A., Gauthier, K. M., Capdevila, J. H., Falck, J. R., Campbell, W. B., & Imig, J. D. (2014). Epoxyeicosatrienoic acid analogue lowers blood pressure through vasodilation and sodium channel inhibition. *Clinical Science*, *127*(7). https://doi.org/10.1042/CS20130479

Kodani, S. D., Wan, D., Wagner, K. M., Hwang, S. H., Morisseau, C., & Hammock, B. D. (2018). Design and Potency of Dual Soluble Epoxide Hydrolase/Fatty Acid Amide Hydrolase Inhibitors. *ACS Omega*, *3*(10). https://doi.org/10.1021/acsomega.8b01625

Kramer, J., & Proschak, E. (2017). Phosphatase activity of soluble epoxide hydrolase. In *Prostaglandins and Other Lipid Mediators* (Vol. 133). https://doi.org/10.1016/j.prostaglandins.2017.07.002

Kujal, P., Čertíková Chábová, V., Škaroupková, P., Husková, Z., Vernerová, Z., Kramer, H. J., Walkowska, A., Kompanowska-Jezierska, E., Sadowski, J., Kitada, K., Nishiyama, A., Hwang, S. H., Hammock, B. D., Imig, J. D., & Červenka, L. (2014). Inhibition of soluble epoxide hydrolase is renoprotective in 5/6 nephrectomized Ren-2 transgenic hypertensive rats. *Clinical and Experimental Pharmacology & Physiology*, *41*(3), 227–237. https://doi.org/10.1111/1440-1681.12204

Kupferberg, A., Bicks, L., & Hasler, G. (2016). Social functioning in major depressive disorder. In *Neuroscience and Biobehavioral Reviews* (Vol. 69). https://doi.org/10.1016/j.neubiorev.2016.07.002

Lazaar, A. L., Yang, L., Boardley, R. L., Goyal, N. S., Robertson, J., Baldwin, S. J., Newby, D. E., Wilkinson, I. B., Tal-Singer, R., Mayer, R. J., & Cheriyan, J. (2016). Pharmacokinetics, pharmacodynamics and adverse event profile of GSK2256294, a novel soluble epoxide hydrolase inhibitor. *British Journal of Clinical Pharmacology*, *81*(5). https://doi.org/10.1111/bcp.12855

Lee, K. S. S., Liu, J. Y., Wagner, K. M., Pakhomova, S., Dong, H., Morisseau, C., Fu, S. H., Yang, J., Wang, P., Ulu, A., Mate, C. A., Nguyen, L. V., Hwang, S. H., Edin, M. L., Mara, A. A., Wulff, H., Newcomer, M. E., Zeldin, D. C., & Hammock, B. D. (2014). Optimized inhibitors of soluble epoxide hydrolase improve in vitro target residence time and in vivo efficacy. *Journal of Medicinal Chemistry*, *57*(16). https://doi.org/10.1021/jm500694p

Lemus-Conejo, A., Millan-Linares, M. del C., Toscano, R., Millan, F., Pedroche, J., Muriana, F. J. G., & Montserrat-de la Paz, S. (2022). GPETAFLR, a peptide from Lupinus angustifolius L. prevents inflammation in microglial cells and confers neuroprotection in brain. *Nutritional Neuroscience*, *25*(3). https://doi.org/10.1080/1028415X.2020.1763058

Li, K., Zhou, G., Xiao, Y., Gu, J., Chen, Q., Xie, S., & Wu, J. (2022). Risk of Suicidal Behaviors and Antidepressant Exposure Among Children and Adolescents: A Meta-Analysis of Observational Studies. In *Frontiers in Psychiatry* (Vol. 13). https://doi.org/10.3389/fpsyt.2022.880496

Li, S. H., Zhao, P., Tian, H. B., Chen, L. H., & Cui, L. Q. (2017). Soluble epoxide hydrolase inhibitor, 12-(3-adamantan-1-yl-ureido)-dodecanoic acid, represses human aortic smooth muscle cell proliferation and migration by regulating cell death pathways via the mTOR signaling. *International Journal of Clinical and Experimental Pathology*, *10*(8).

Lotrich, F. E., El-Gabalawy, H., Guenther, L. C., & Ware, C. F. (2011). The role of inflammation in the pathophysiology of depression: different treatments and their effects. *The Journal of Rheumatology. Supplement*, *88*(SUPPL. 88), 48–54. https://doi.org/10.3899/JRHEUM.110903

Lukin, A., Kramer, J., Hartmann, M., Weizel, L., Hernandez-Olmos, V., Falahati, K., Burghardt, I., Kalinchenkova, N., Bagnyukova, D., Zhurilo, N., Rautio, J., Forsberg, M., Ihalainen, J., Auriola, S., Leppänen, J., Konstantinov, I., Pogoryelov, D., Proschak, E., Dar'in, D., & Krasavin, M. (2018). Discovery of polar spirocyclic orally bioavailable urea inhibitors of soluble epoxide hydrolase. *Bioorganic Chemistry*, *80*. https://doi.org/10.1016/j.bioorg.2018.07.014

Mahapatra, A. Das, Choubey, R., & Datta, B. (2020). Small molecule soluble epoxide hydrolase inhibitors in multitarget and combination therapies for inflammation and cancer. *Molecules*, *25*(23). https://doi.org/10.3390/molecules25235488

Maniar, K. H., Jones, I. A., Gopalakrishna, R., & Vangsness, C. T. (2018). Lowering side effects of NSAID usage in osteoarthritis: recent attempts at minimizing dosage. In *Expert Opinion on Pharmacotherapy* (Vol. 19, Issue 2). https://doi.org/10.1080/14656566.2017.1414802

Manickam, M., Pillaiyar, T., Boggu, P., Venkateswararao, E., Jalani, H. B., Kim, N. D., Lee, S. K., Jeon, J. S., Kim, S. K., & Jung, S. H. (2016). Discovery of enantioselectivity of urea inhibitors of soluble epoxide hydrolase. *European Journal of Medicinal Chemistry*, *117*. https://doi.org/10.1016/j.ejmech.2016.04.015

McMasters, J., Poh, S., Lin, J. B., & Panitch, A. (2017). Delivery of anti-inflammatory peptides from hollow PEGylated poly(NIPAM) nanoparticles reduces inflammation in an ex vivo osteoarthritis model. *Journal of Controlled Release*, *258*. https://doi.org/10.1016/j.jconrel.2017.05.008

Morisseau, C., Du, G., Newman, J. W., & Hammock, B. D. (1998). Mechanism of mammalian soluble epoxide hydrolase inhibition by chalcone oxide derivatives. *Archives of Biochemistry and Biophysics*, *356*(2). https://doi.org/10.1006/abbi.1998.0756

Morisseau, C., Goodrow, M. H., Dowdy, D., Zheng, J., Greene, J. F., Sanborn, J. R., & Hammock, B. D. (1999). Potent urea and carbamate inhibitors of soluble epoxide hydrolases. *Proceedings of the National Academy of Sciences of the United States of America*, *96*(16). https://doi.org/10.1073/pnas.96.16.8849

Morisseau, C., Goodrow, M. H., Newman, J. W., Wheelock, C. E., Dowdy, D. L., & Hammock, B. D. (2002). Structural refinement of inhibitors of urea-based soluble epoxide hydrolases. *Biochemical Pharmacology*, *63*(9). https://doi.org/10.1016/S0006-2952(02)00952-8

Morisseau, C., & Hammock, B. D. (2005). Epoxide hydrolases: Mechanisms, inhibitor designs, and biological roles. In *Annual Review of Pharmacology and Toxicology* (Vol. 45). https://doi.org/10.1146/annurev.pharmtox.45.120403.095920

Njeim, R., Braych, K., Ghadieh, H. E., Azar, N. S., Azar, W. S., Dia, B., Leone, A., Cappello, F., Kfoury, H., Harb, F., Jurjus, A. R., Eid, A. A., & Ziyadeh, F. N. (2023). VEGF-A: A Novel Mechanistic Link Between CYP2C-Derived EETs and Nox4 in Diabetic Kidney Disease. *Diabetes*, *72*(7). https://doi.org/10.2337/db22-0636

Nuthikattu, S., Milenkovic, D., Norman, J. E., Rutledge, J., & Villablanca, A. (2021). Inhibition of soluble epoxide hydrolase is protective against the multiomic effects of a high glycemic diet on brain microvascular inflammation and cognitive dysfunction. *Nutrients*, *13*(11). https://doi.org/10.3390/nu13113913

Pecic, S., Zeki, A. A., Xu, X., Jin, G. Y., Zhang, S., Kodani, S., Halim, M., Morisseau, C., Hammock, B. D., & Deng, S. X. (2018). Novel piperidine-derived amide sEH inhibitors as mediators of lipid metabolism with improved stability. *Prostaglandins and Other Lipid Mediators*, *136*. https://doi.org/10.1016/j.prostaglandins.2018.02.004

Rand, A. A., Barnych, B., Morisseau, C., Cajka, T., Lee, K. S. S., Panigrahy, D., & Hammock, B. D. (2017). Cyclooxygenase-derived proangiogenic metabolites of epoxyeicosatrienoic acids. *Proceedings of the National Academy of Sciences of the United States of America*, *114*(17). https://doi.org/10.1073/pnas.1616893114

Rezaee, E., Amrolah, S. M., Nazari, M., & Tabatabai, S. A. (2021). Novel amide derivatives of 3-phenylglutaric acid as potent soluble epoxide hydrolase inhibitors. *Molecular Diversity*, *25*(1). https://doi.org/10.1007/s11030-019-10023-y

Rieffe, C., & De Rooij, M. (2012). The longitudinal relationship between emotion awareness and internalising symptoms during late childhood. *European Child and Adolescent Psychiatry*, *21*(6). https://doi.org/10.1007/s00787-012-0267-8

Santomauro, D. F., Mantilla Herrera, A. M., Shadid, J., Zheng, P., Ashbaugh, C., Pigott, D. M., Abbafati, C., Adolph, C., Amlag, J. O., Aravkin, A. Y., Bang-Jensen, B. L., Bertolacci, G. J., Bloom, S. S., Castellano, R., Castro, E., Chakrabarti, S., Chattopadhyay, J., Cogen, R. M., Collins, J. K., Ferrari, A. J. (2021). Global prevalence and burden of depressive and anxiety disorders in 204 countries and territories in 2020 due to the COVID-19 pandemic. *The Lancet*, *398*(10312). https://doi.org/10.1016/S0140-6736(21)02143-7

Sasso, O., Wagner, K., Morisseau, C., Inceoglu, B., Hammock, B. D., & Piomelli, D. (2015). Peripheral FAAH and soluble epoxide hydrolase inhibitors are synergistically antinociceptive. *Pharmacological Research*, *97*. https://doi.org/10.1016/j.phrs.2015.04.001

Schäfer, A., Neschen, S., Kahle, M., Sarioglu, H., Gaisbauer, T., Imhof, A., Adamski, J., Hauck, S. M., & Ueffing, M. (2015). The epoxyeicosatrienoic acid pathway enhances hepatic insulin signaling and is repressed in insulin-resistant mouse liver. *Molecular and Cellular Proteomics*, *14*(10). https://doi.org/10.1074/mcp.M115.049064

Shen, H. C., & Hammock, B. D. (2012). Discovery of inhibitors of soluble epoxide hydrolase: A target with multiple potential therapeutic indications. In *Journal of Medicinal Chemistry* (Vol. 55, Issue 5). https://doi.org/10.1021/jm201468j

Sun, C.-P., Zhang, X.-Y., Morisseau, C., Hwang, S. H., Zhang, Z.-J., Hammock, B. D., & Ma, X.-C. (2021). Discovery of Soluble Epoxide Hydrolase Inhibitors from Chemical Synthesis and Natural Products. *Journal of Medicinal Chemistry*, *64*(1), 184–215. https://doi.org/10.1021/acs.jmedchem.0c01507

Sung, H. H., Tsai, H. J., Liu, J. Y., Morisseau, C., & Hammock, B. D. (2007). Orally bioavailable potent soluble epoxide hydrolase inhibitors. *Journal of Medicinal Chemistry*, *50*(16). https://doi.org/10.1021/jm070270t

Swardfager, W., Hennebelle, M., Yu, D., Hammock, B. D., Levitt, A. J., Hashimoto, K., & Taha, A. Y. (2018). Metabolic/inflammatory/vascular comorbidity in psychiatric disorders; soluble epoxide hydrolase (sEH) as a possible new target. *Neuroscience and Biobehavioral Reviews*, *87*, 56–66. https://doi.org/10.1016/J.NEUBIOREV.2018.01.010

Tarkany Basting, R., Henrique Napimoga, M., Antônio Trindade Silva, C., Ballassini Abdalla, H., Campos Durso, B., Henrique Barboza Martins, L., de Abreu Cavalcanti, H., Hammock, B. D., & Trindade Clemente-Napimoga, J. (2023). Soluble epoxide hydrolase inhibitor blockage microglial cell activation in subnucleus caudalis in a persistent model of arthritis. *International Immunopharmacology*, *120*, 110320. https://doi.org/10.1016/J.INTIMP.2023.110320

Tsai, H. J., Hwang, S. H., Morisseau, C., Yang, J., Jones, P. D., Kasagami, T., Kim, I. H., & Hammock, B. D. (2010). Pharmacokinetic screening of soluble epoxide hydrolase inhibitors in dogs. *European Journal of Pharmaceutical Sciences*, *40*(3). https://doi.org/10.1016/j.ejps.2010.03.018

Udenigwe, C. C., Abioye, R. O., Okagu, I. U., & Obeme-Nmom, J. I. (2021). Bioaccessibility of bioactive peptides: recent advances and perspectives. In *Current Opinion in Food Science* (Vol. 39). https://doi.org/10.1016/j.cofs.2021.03.005

Varcabova, S., Huskova, Z., Kramer, H. J., Hwang, S. H., Hammock, B. D., Imig, J. D., Kitada, K., & Cervenka, L. (2013). Antihypertensive action of soluble epoxide hydrolase inhibition in Ren-2 transgenic rats is mediated by suppression of the intrarenal renin–angiotensin system. *Clinical and Experimental Pharmacology and Physiology*, *40*(4), 273–281. https://doi.org/10.1111/1440-1681.12018

Wang, B., Wu, L., Chen, J., Dong, L., Chen, C., Wen, Z., Hu, J., Fleming, I., & Wang, D. W. (2021). Metabolism pathways of arachidonic acids: mechanisms and potential therapeutic targets. In *Signal Transduction and Targeted Therapy* (Vol. 6, Issue 1). https://doi.org/10.1038/s41392-020-00443-w

Weightman, M. J., Knight, M. J., & Baune, B. T. (2019). A systematic review of the impact of social cognitive deficits on psychosocial functioning in major depressive disorder and opportunities for therapeutic intervention. *Psychiatry Research*, *274*. https://doi.org/10.1016/j.psychres.2019.02.035

WHO. (2019). https://www.who.int/news-room/fact-sheets/detail/depression. *International Immunopharmacology*, *67*(August 2018).

Wu, C. H., Shyue, S. K., Hung, T. H., Wen, S., Lin, C. C., Chang, C. F., & Chen, S. F. (2017). Genetic deletion or pharmacological inhibition of soluble epoxide hydrolase reduces brain

damage and attenuates neuroinflammation after intracerebral hemorrhage. *Journal of Neuroinflammation*, *14*(1). https://doi.org/10.1186/S12974-017-1005-4

Yang, L., Mäki-Petäjä, K., Cheriyan, J., McEniery, C., & Wilkinson, I. B. (2015). The role of epoxyeicosatrienoic acids in the cardiovascular system. *British Journal of Clinical Pharmacology*, *80*(1). https://doi.org/10.1111/bcp.12603

Yu, Z., Xu, F., Huse, L. M., Morisseau, C., Draper, A. J., Newman, J. W., Parker, C., Graham, L. R., Engler, M. M., Hammock, B. D., Zeldin, D. C., & Kroetz, D. L. (2000). Soluble epoxide hydrolase regulates hydrolysis of vasoactive epoxyeicosatrienoic acids. *Circulation Research*, *87*(11). https://doi.org/10.1161/01.RES.87.11.992

Zhang, C. Y., Tan, X. H., Yang, H. H., Jin, L., Hong, J. R., Zhou, Y., & Huang, X. T. (2022). COX-2/sEH Dual Inhibitor Alleviates Hepatocyte Senescence in NAFLD Mice by Restoring Autophagy through Sirt1/PI3K/AKT/mTOR. *International Journal of Molecular Sciences*, *23*(15). https://doi.org/10.3390/ijms23158267

Zhang, D., Ai, D., Tanaka, H., Hammock, B. D., & Zhu, Y. (2010). DNA methylation of the promoter of soluble epoxide hydrolase silences its expression by an SP-1-dependent mechanism. *Biochimica et Biophysica Acta*, *1799*(9), 659–667. https://doi.org/10.1016/J.BBAGRM.2010.09.006

Zhang, H., Hu, C. A. A., Kovacs-Nolan, J., & Mine, Y. (2015). Bioactive dietary peptides and amino acids in inflammatory bowel disease. *Amino Acids*, *47*(10). https://doi.org/10.1007/s00726-014-1886-9

Zhang, J., Zhang, W.-H., Morisseau, C., Zhang, M., Dong, H.-J., Zhu, Q.-M., Huo, X.-K., Sun, C.-P., Hammock, B. D., & Ma, X.-C. (2023). Genetic deletion or pharmacological inhibition of soluble epoxide hydrolase attenuated particulate matter 2.5 exposure mediated lung injury. *Journal of Hazardous Materials*, 131890. https://doi.org/10.1016/j.jhazmat.2023.131890

Zimmerman, M., Balling, C., Chelminski, I., & Dalrymple, K. (2018). Understanding the severity of depression: Which symptoms of depression are the best indicators of depression severity? *Comprehensive Psychiatry*, *87*. https://doi.org/10.1016/j.comppsych.2018.09.006

CHAPTER 2 – BIOMOLECULAR INTERACTIONS AND INHIBITION KINETICS OF HUMAN SOLUBLE EPOXIDE HYDROLASE BY TETRAPEPTIDE YMSV

Joy I. Obeme-Nmom[1], Raliat O. Abioye[1], Toluwase H. Fatoki[2], Chibuike C. Udenigwe[1,3 *]

[1]Department of Chemistry and Biomolecular Sciences, Faculty of Science, University of Ottawa, Ottawa, ON K1N 6N5, Canada.

[2]Department of Biochemistry, Federal University Oye-Ekiti, PMB 373, Oye-Ekiti, Ekiti State, Nigeria.

[3]School of Nutrition Sciences, Faculty of Health Sciences, University of Ottawa, Ottawa. ON K1H 8M5, Canada.

https://doi.org/10.31665/JFB.2023.18341

Abstract

Soluble epoxide hydrolase (sEH) contributes to the pathophysiology of neurodegenerative diseases by decreasing the epoxyeicosatrienoic acids/dihydroeicosatrienoic acids ratio and influencing the anti-inflammatory system. Thus, sEH inhibition reduces systemic inflammation, particularly in the brain. This study investigated sEH inhibition by a tetrapeptide, YMSV, and its mechanism of action. Enzyme inhibition kinetics demonstrated that YMSV is a mixed-competitive inhibitor of sEH, with a half-maximal inhibitory concentration (IC_{50}) of 179.5 ± 0.92 μM. Secondary structural analysis of sEH by circular dichroism showed that YMSV decreased the α-helices by 7.7% and increased the β-sheets and random coils by 11.4% and 22%, respectively. Molecular docking simulation indicated that YMSV formed a hydrogen bond with the Asp333 residue of the hydrolase pocket of sEH in addition to the binding of non-active site residues. The findings provide new insights into the mechanism of sEH inhibition by YMSV and its potential as a peptide-based anti-depressant nutraceutical.

Keywords: soluble epoxide hydrolase (sEH), enzyme inhibition kinetics, bioactive peptides, EET, DHET, biomolecular interaction

2.1. Introduction

Soluble epoxide hydrolase (sEH) has been studied extensively for its preclinical and clinical importance and implications in several diseases. sEH is involved in the metabolic transformation of epoxides into less active diols. It is predominantly expressed in the liver, brain, kidney, heart, lung, spleen, adrenal, and gut, where it plays a role in systemic inflammation and blood pressure regulation. Within the cell, sEH is found in the peroxisome, membrane, and cytosol (Hollinshead & Meijer, 1988). The 120-kDa homodimer enzyme belongs to the α/β-hydrolase fold superfamily and catalyzes the hydrolysis of epoxides using its C-terminal domain and the hydrolysis of phospholipids using the N-terminal domain (Morisseau & Hammock, 2013). sEH substrates are biologically important epoxides known as epoxyeicosatrienoic acids (EETs), which are derived from arachidonic acid metabolism in the cytochrome P450 pathway. Hydrolysis of EETs by sEH into the less active dihydroeicosatrienoic acids (DHETs) fundamentally affects the overall regulation of epoxy fatty acids (EpFAs) and inflammation in the body (Swardfager et al., 2018). EETs are signaling molecules that are prevalently abundant in the liver, smooth muscles, and blood vessels of other major organs. Their functions in cardio protection, fibrinolysis, smooth muscle migration, angiogenesis, vasodilation and prevention of inflammation, apoptosis, and oxidation can be attributed to various mechanisms such as decreased TNF-α secretion in monocytic cells, inhibition of ICAM-1, VCAM-1, and E-selectin expression, and obstruction of NF-κB nuclear translocation, which in turn downregulates several enzymes, including inducible nitric oxide synthase (iNOS) (Khan et al., 2013). Consequently, sEH has attracted notable attention due to the wide variety of therapeutic potential shown by EETs, especially in cardiovascular, neurodegenerative, and metabolic diseases (Sun et al., 2021).

Bioactive peptides are a sequence of 2-20 amino acids that have beneficial health-promoting properties, including anti-inflammatory, antioxidant, anticancer, antihypertensive, antimicrobial, and immunomodulatory activities. The biological functions of these peptides make them important candidates for pharmaceutical and therapeutic treatments for various diseases, such as diabetes, hypertension, and neurodegenerative diseases (Udenigwe et al., 2021). Several *in vivo* and *in vitro* studies have demonstrated the anti-inflammatory effects of food-derived bioactive peptides. Peptides derived from eggs, milk, and soybean have expressed anti-inflammation by reducing the expressions of TNF-κ, IL-10, IL-6, IL-1β, ICAM-1 and VCAM-1 as well as inhibition of nitric oxide production (Guha & Majumder, 2019). Specifically, bioactive peptides from milk and soy

proteins have been reported to inhibit the NF-κB pathway by decreasing the levels of NF-κB in the cell nucleus and increasing the concentration of IκB concentration in the cytosol, which led to Nrf2 activation, and the expression of IL-1ra (interleukin-1 receptor antagonist protein) which is an anti-inflammatory cytokine (Tonolo et al., 2022). Similar mechanisms have been reported for EETs; thus, the bioactive peptides can be applied in improving the inflammation response of the body.

The pharmacophore of many first chemically synthesized SEH inhibitors, such as 12-(3-adamantan-1-yl-ureido) dodecanoic acid (AUDA), involve the incorporation of urea analogues and amide groups to produce a similar configuration as the epoxide while employing an arachidonic acid backbone as the model structure. Multitarget inhibitors of sEH and other enzymes and receptors involved in the inflammatory pathway, such as COX-2, FAAH, and PPAR, have been discovered (Iyer et al., 2022; Sun et al., 2021). The dual sEH inhibitor *t*-TUCB has been described as a poor inhibitor of FAAH (Kodani et al., 2018); PTUPB also interacts with the histidine and tyrosine residues of the COX-2 active site by hydrogen bonding (Hwang et al., 2011; Zhang et al., 2014); AUBPC and TPUBPC are effectors designed to inhibit sEH while activating PPAR α/γ (Buscató et al., 2012). Naturally derived sEH inhibitors have also been identified in various plants, including flavonoids from Capsicum Chinese jacq. Cv. Habanero (Kim et al., 2019), phenolic compounds from Vietnam's *Passiflora edulis* seeds (Cuong et al., 2019), anthraquinone and stilbene derivatives from *Rheum undulatum* (Jo et al., 2016), as well as triterpenes and phenylpropanoid derivatives from *Lycopus lucidus* roots (Han et al., 2021). However, these natural sEH inhibitors have poor pharmacokinetics properties, including low water solubility, absorption in the gastrointestinal tract, and bioaccessibility (Lee et al., 2020). In addition to the amide group pharmacophore, many bioactive peptides are relatively stable with good pharmacokinetics properties, and some have the ability to penetrate the blood-brain barrier (BBB), thus the possibility of their development as sEH inhibitors and anti-depressive nutraceuticals. This study was conducted with the goal of determining the mechanisms of inhibition and biomolecular interactions of tetrapeptide YMSV as an inhibitor of soluble epoxide hydrolase.

2.2 Materials and Method

2.2.1. Materials and reagents

Human soluble epoxide hydrolase and 3-phenyl-cyano(6-methoxy-2-naphthalenyl) methylester-2-oxirane acetic acid (PHOME) were purchased from Cayman Chemical (Ann Arbor, Michigan, USA). Peptide YMSV was synthesized with a purity of over 95% by GenScript Inc. (New Jersey, USA). Bovine serum albumin (BSA), bis-Tris-HCl, 6-methoxy-2-naphthaldehyde (6M2N), and dimethyl sulfoxide (DMSO) were purchased from MilliporeSigma (Oakville, ON, Canada). All the chemical reagents are analytical grade and used without further purification.

2.2.2. sEH inhibition assay

The *in vitro* inhibition of soluble epoxide hydrolase by YMSV peptide was conducted by a fluorometric assay using 3-phenyl-cyano(6-methoxy-2-naphthalene) methyl ester-2-oxirane acetic acid (PHOME) as previously described with some modifications (Abis et al., 2019a; Kim et al., 2019). Briefly, 50 µL of 16 ng/mL human sEH in the reaction buffer (25 mM bis-Tris-HCl buffer, pH 7.0, containing 0.1% BSA), and 50 µL of peptide YMSV (6.25–250 µM, in reaction buffer) were mixed in a black 96-well plate, followed by the addition of 50 µL of the buffer containing 5 µM PHOME. The appearance of the fluorometric product, 6-methoxy-2-naphthaldehyde (6M2N) was then measured as relative fluorescence unit (RFU) for 1 h using the Spark multimode microplate reader (Tecan, Stockholm, Sweden), with the following setup: excitation wavelength 330 nm, emission wavelength 460 nm, detection every 45 s, gain 750, and 30 °C constant temperature. The reaction rate (RFU/min) was calculated as:

$$Rate = \frac{S_F - C_F}{\Delta t}$$

S_F and C_F are the fluorescence intensities of the assay mixture in the presence and absence of the inhibitor, respectively over 1 h of enzyme assay. The inhibitory activity of sEH was calculated using the equation:

$$\%\ Inhibitory\ activity = 1 - \left(\frac{\Delta F_{sample}}{\Delta F_{control}}\right) \times\ 100$$

ΔF_{sample} and $\Delta F_{control}$ are changes in the fluorescence intensity in the presence and absence of the inhibitor, respectively over 1 h of enzyme assay.

The IC_{50}, the concentration of the inhibitor that reduced the activity of sEH by 50%, was determined using the linear regression obtained from the curve of the percent inhibition vs. inhibitor concentration.

2.2.3. Enzyme inhibition Kinetics studies

The kinetics of sEH-catalyzed conversion of PHOME to 6-methoxy-2-naphthaldehyde was studied within the first 30 mins of the enzyme assay in the absence and presence of 25-250 μM YMSV at 1.25, 2.5, 5, 10 and 20 μM PHOME, a range previously reported for sEH kinetics studies (Jo et al., 2016). The mode of inhibition was determined by Lineweaver-Burk plot and enzymatic kinetics parameters (K_m and V_{max}) were determined from Lineweaver-Burk plot using GraphPad Prism version 9.1.2 for Windows (GraphPad Software, La Jolla, CA, USA). To test for the effect of substrate (PHOME) on sEH inactivation in the presence and absence of YMSV, the kinetics assay was carried out for 6 h to determine kinetic inactivation parameters (P_∞ and apparent inactivation rate constant, *A*). The concentration of the product (6M2N) released by sEH was determined using a standard curve of 6M2N.

2.2.4. Circular dichroism spectroscopy

The effect of YMSV on the secondary structure of human sEH was examined using the Jasco J-715 circular dichroism spectrophotometer (Jasco Corp., Tokyo, Japan). Measurements were performed at a human sEH/YMSV molar ratio of 1:1 with a final human sEH concentration of 64 ng/mL and YMSV concentration of 250 μM in 100 mM phosphate buffer (pH 7.4). The final reaction volume of 250 μL was incubated for 5 min at 30 °C. Measurements were carried out at room temperature in nitrogen gas using a quartz cuvette with a path length of 1 mm. Three scans were recorded and averaged with the wavelength ranging from 185 to 280 nm at a scanning speed of 50 nm/s. Phosphate buffer was used as blank to perform baseline subtraction of the spectral output, and the result was translated into mean residue ellipticity (deg cm^2 $dmol^{-1}$) using a mean residue weight of 64 kDa and a human sEH concentration of 0.025 mg/mL. All data processing was carried out using CDToolX (Miles & Wallace, 2018). The data acquired were plotted using GraphPad Prism version 9.1.2 for Windows (GraphPad Software, La Jolla, CA, USA). Bestsel, a software for CD fitting, was used to calculate the secondary structure contents using a wavelength range of 190-250 nm (Micsonai et al., 2018).

2.2.5. Molecular docking simulation

Molecular docking studies were carried out with human sEH and YMSV. Briefly, human sEH structure (PDB ID: 3otq) was obtained from www.rcsb.org/pdb. YMSV sequence was converted to SMILES (Simplified Molecular Input Line Entry Specification) format using PepSMI (https://www.novoprolabs.com/tools/convert-peptide-to-smiles-string) and the SMILES string was converted to PDB format using SwissTargetPrediction (http://www.swisstargetprediction.ch/) (Daina et al., 2017). PyMol software was used to prepare the protein by the removal of water and existing ligands. Both YMSV (ligand) and human sEH protein were prepared for docking using AutoDock Tools (ADT) v1.5.6 (Morris et al., 2009) at default settings, and the output file was saved in pdbqt format. Active site amino acid residues of the enzyme were obtained from the literature (Schiøtt & Bruice, 2002) and used to define the docking parameters: center grid box (78.369 × -7.222 × 65.775 points), size (70 × 70 × 70 points), and spacing (0.375 Å). The molecular docking program AutoDock Vina v1.2.3 (Eberhardt et al., 2021; Trott & Olson, 2010) was employed for the docking experiment (Rentzsch & Renard, 2015). After docking, close interactions of binding of the target with the ligands were analyzed and visualized using PyMol and ezLigPlot(Tao et al., 2019).

2.2.6. ADME analysis

The ADME/Tox properties of peptide YMSV and sEH inhibitor, AUDA, were analyzed and compared. SMILES strings of the peptide were obtained using PepSMI (https://www.novoprolabs.com/tools/convert-peptide-to-smiles-string) while that of AUDA was obtained from the NCBI PubChem Compound database (http://www.pubchem.ncbi.nlm.nih.gov/compound). Pharmacokinetics and drug-likeness were determined using SwissADME, https://www.swissadme.ch/index (Daina et al., 2017), which predicts the absorption, distribution, metabolism, and excretion properties of compounds.

2.2.7. Statistical analysis

Enzyme inhibition experiments were done in triplicate and data were presented as mean ± standard deviation. Statistical analysis was performed with GraphPad Prism version 9.1.2 for Windows (GraphPad Software, La Jolla, CA, USA) using Tukey's or Dunnett's multiple comparisons tests with a significance level set at $p < 0.05$.

2.3. Results and Discussion

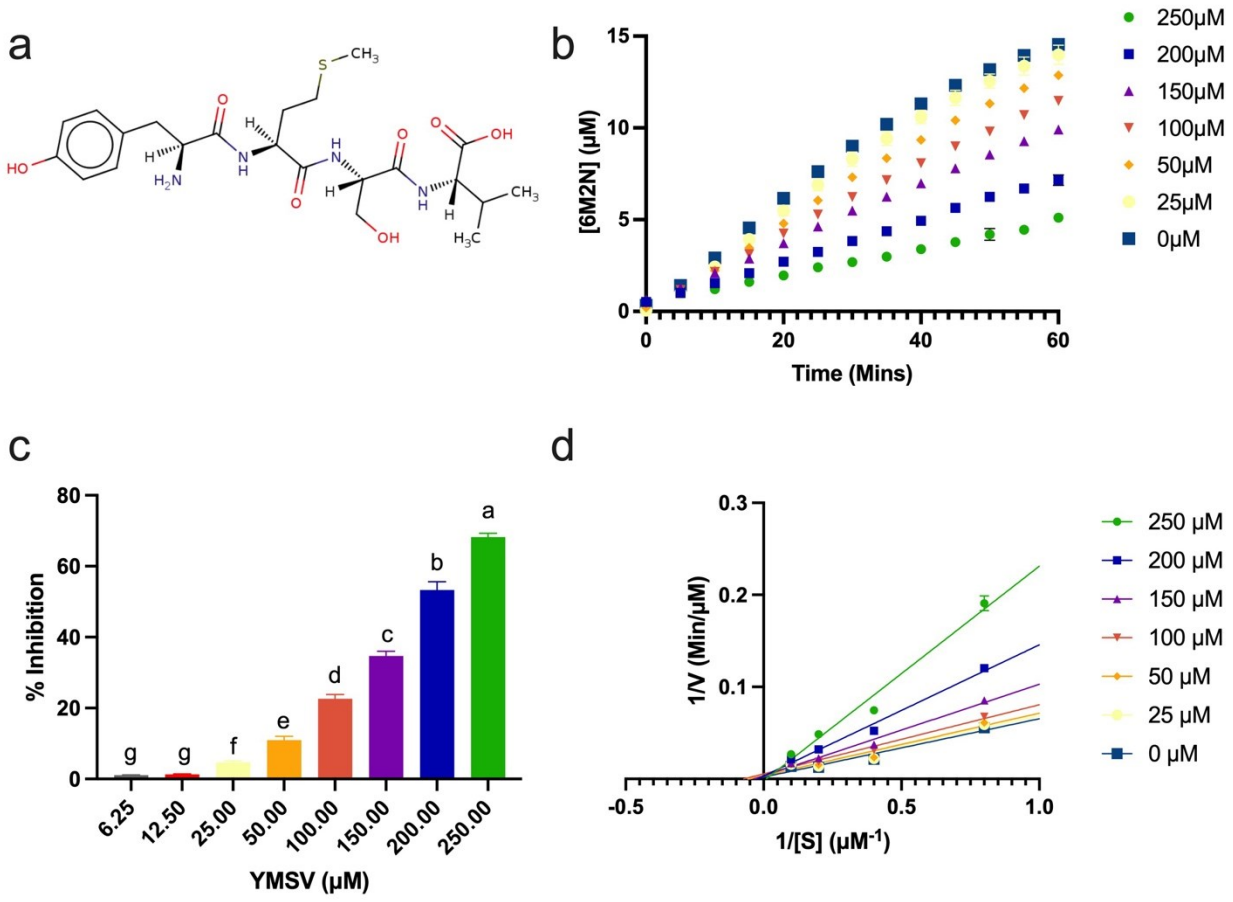

Figure 2.1. Effect of YMSV on the activity of soluble epoxide hydrolase (sEH). (A) Structure of peptide YMSV; (B) plots of the product (6M2N) formed at constant [S] (5 μM PHOME) over time at different concentrations of the inhibitor, YMSV; (C) concentration-dependent sEH inhibitory activity of YMSV; (D) Lineweaver-Burk double reciprocal plot of sEH at different YMSV concentration.

2.3.1 sEH reaction kinetics and inhibition mode of YMSV

Previous studies have shown that compounds containing urea or amide backbones are excellent and stable inhibitors of human and mouse sEH (Sun et al., 2021). This feature is present in peptides, making them strong sEH inhibitor candidates. Screening of several peptides from our library for sEH inhibition resulted in the selection of YMSV for further studies. YMSV occurs naturally in food proteins, e.g., castor bean (*Ricinus communis*) protein disulfide-isomerase (f181-184; accession no. Q43116 (PDI_RICCO). Enzyme assays with YMSV (Figure 1A) showed a decrease in the sEH reaction rate (Figure 1B). Concentration-dependent inhibition of sEH by YMSV was apparent at inhibitor concentrations of 25 to 250 μM, with negligible effect at lower concentrations (Figure 1C). The half maximal inhibitory concentration (IC_{50}) was estimated to be 178.5 ± 0.92 μM. A recent study with corn gluten-derived tripeptides WEY, WWY, WYW, YFW and YFY showed lower sEH inhibiting IC_{50} values ranging from 55.41 to 96 μM (Dang et al., 2022). The higher YMSV IC_{50} value could be attributed to its larger size and length, compared to the tripeptides, as the size of the latter could facilitate binding to sEH, or specific favorable binding conformation. Molecular size plays an important role in sEH inhibition since the narrow cavity of the enzyme active site might limit access to large and bulky inhibitors (Dang et al., 2022). The aromatic amino acid residues can readily participate in hydrogen bonding because of their -OH and -NH functional groups, and as nucleophiles at the enzyme active site (Scheiner et al., 2002). The tripeptides containing aromatic residues showed high sEH inhibitory activity up to 70% at 100 μM concentration, especially YFW and YFY, which had the highest IC_{50} values (Dang et al., 2022). Notably, the tripeptides have a common aromatic amino acid residue, tyrosine, as YMSV, suggesting a similarity in their interactions with sEH.

A standard curve was prepared using 6M2N to determine the amount of product formed by sEH and the peptide inhibitory effects after 60 min. The rate of the product formed over time at 5 μM substrate and varying concentrations of YMSV is shown in Figure 1B. The concentration of YMSV is inversely correlated with the concentration of the product formed, with a 68% decrease at the highest YMSV concentration.

Table 2.1. Kinetics parameters of sEH catalyzed reaction in the absence and presence of different concentrations of the YMSV peptide.

YMSV (μM)	V_{max} (μM/min)	K_m (μM)
0	110.30 ± 0.36	3.514 ± 0.02
25	89.31 ± 4.55***	2.928 ± 0.11^{ns}
50	90.06 ± 1.29***	3.216 ± 0.05^{ns}
100	91.42 ± 1.54***	4.648 ± 0.17^{ns}
150	103.60 ± 0.90^{ns}	7.375 ± 0.14**
200	98.61 ± 0.66*	11.037 ± 0.16****
250	128.43 ± 9.92***	24.830 ± 2.80****

K_m, Michaelis constant in the absence and presence of the inhibitor; V_{max}, maximum reaction velocity in the absence and presence of the inhibitor; ns, not significant ($p \geq 0.05$); *, significant at $0.01 > p > 0.05$); **, significant at $0.01 > p > 0.001$; *, significant at $0.001 > p > 0.0001$; ****, significant at $p < 0.0001$ compared to control sEH (at 0 μM inhibitor)**

Lineweaver-Burk plots were used to determine the mode of sEH inhibition by YMSV. Double reciprocal plots of sEH-catalyzed reactions in the presence and absence of YMSV are shown in Figure 1D. The K_m value of sEH activity without YMSV was determined to be 3.514 ± 0.02 μM. At lower inhibitor concentrations, the K_m values were similar to that of the uninhibited enzyme, indicating that sEH had preferred binding affinity for its substrate, although significant inhibition was observed at these concentrations (Figure 1C). This implies that YMSV likely interacted with the enzyme at other regulatory sites or the enzyme-substrate complex, leading to inhibitory activities. However, higher concentrations of the inhibitor increased the K_m of the enzyme. This implies that YMSV was able to competitively bind at sEH active site in place of the substrate, signifying a reduction of substrate affinity. Based on the Lineweaver-Burk plots at varying peptide concentrations, YMSV was shown to be a predominantly competitive inhibitor of sEH (Figure 1D). However, the small but notable changes to the V_{max} of the enzyme (Table 1) suggest it to be

a mixed-competitive inhibitor. This inhibition mode is similar to that reported for martynoside, a phenylpropanoid isolated from the root of *Lycopus lucidus* (Y. K. Han et al., 2021).

2.3.2. Dependence on substrate concentration for product formation

Product formation by sEH increased with time in a substrate-dependent manner over the concentration range of YMSV (Figure 2). In addition, the [S] influenced the value of P_∞ which is the concentration at which the product remains constant. The concentration of P_∞ was inversely proportional to [S]. It is also expected that P_∞ would decrease in the presence of the inhibitor given that product formation is reduced in a concentration-dependent manner.

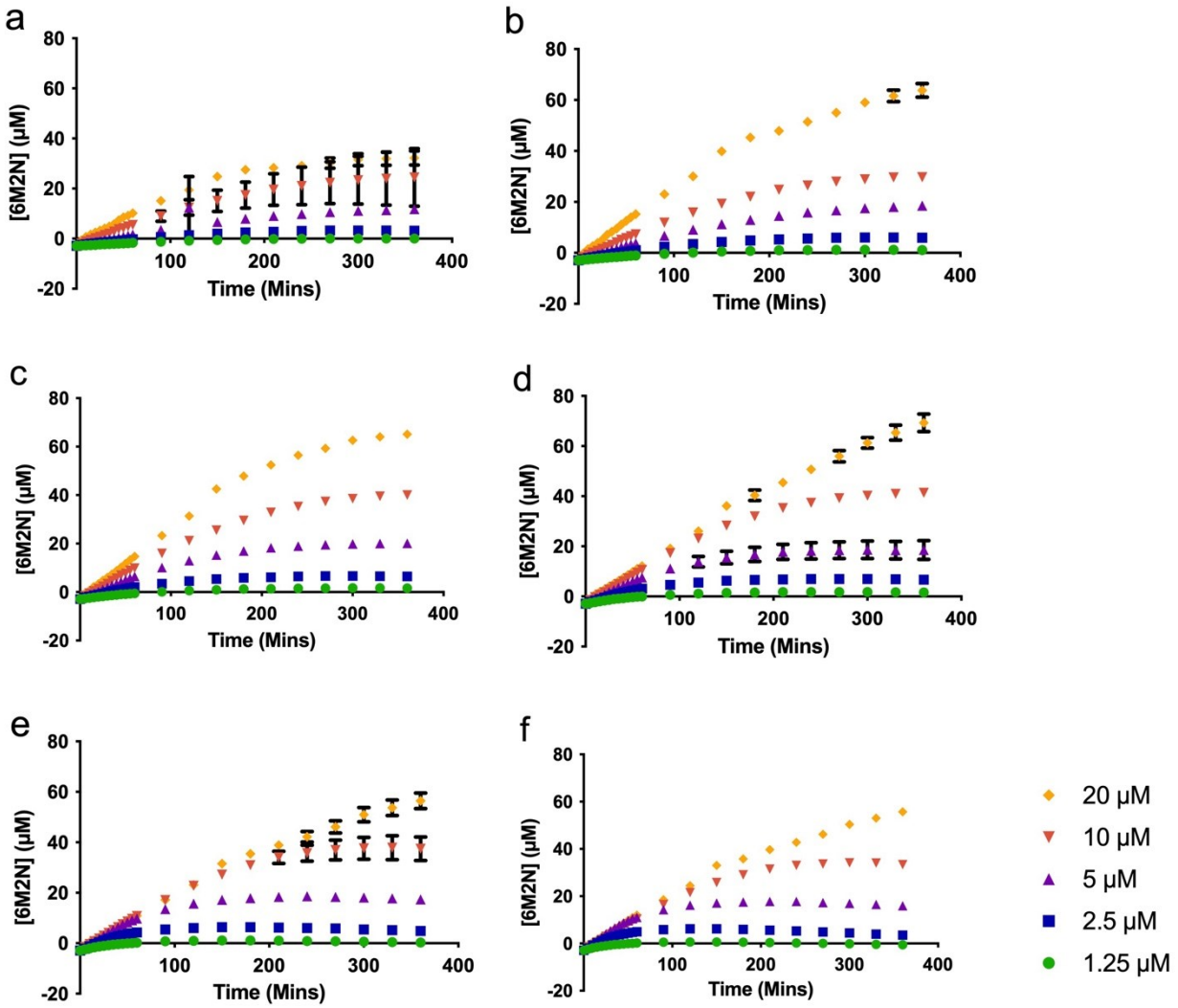

Figure 2.2. Plots of the product (6M2N) formed by human soluble epoxide hydrolase at the substrate (PHOME) concentrations of 1.25-20 µM in the presence of (A) 250 µM (B) 200 µM (C) 150 µM (D) 100 µM (E) 50 µM (F) 25 µM inhibitor (YMSV).

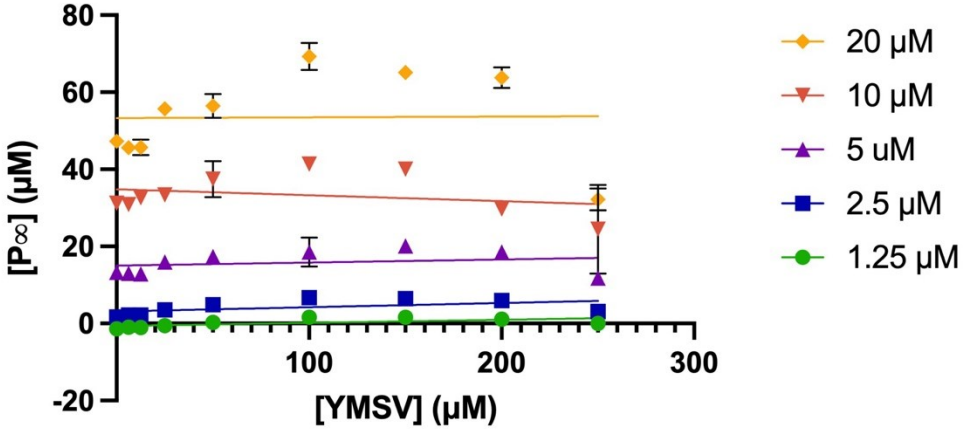

Figure 2.3. Plots of P_∞ against varying concentrations of the inhibitor, YMSV with changing [S] (PHOME = 1.25-20 µM).

As shown in Figure 3, an increase was observed in P_∞ as the concentration of YMSV increased from 25-100 µM, after which P_∞ started decreasing as more YMSV was added to the enzyme reaction at 10 and 20 µM PHOME. This trend was not observed at lower [S] of 1.25-5 µM PHOME where there was no change in P_∞ across all concentrations of YMSV used. This is because most of the substrates were converted into products, resulting in similar P_∞ across all the inhibitor concentrations. In addition, lower [S] makes it easier for YMSV to outcompete the substrate for binding to sEH active site, allowing for higher inhibition and reduced P_∞. Based on this mechanism, at higher [S] (>10 µM), PHOME would overcome the inhibitory effects of YMSV at lower inhibitor concentrations (<100 µM), resulting in a steady increase in P_∞. This suggests that higher [S] promoted binding between the enzyme and substrate, thereby favoring product formation instead of enzyme inhibition by YMSV. The higher concentrations of YMSV resulted in a decrease in P_∞, confirming that sEH inhibition occurred by partly decreasing its affinity for the substrate.

2.3.3. Apparent inactivation rate constant, A and the protective effect of substrate on inactivation

The apparent inactivation constant, A is obtained by taking the slope of the plot of $\ln([P]_\infty - [P])$ vs. time. The plots showed a linear regression with slopes that were dependent on inhibitor concentration (Figure 2.4). At the lowest concentration of YMSV, the first-order kinetics with negative slopes was observed at lower [S] (<5 µM), while zero-order kinetics was observed at high [S] (>10 µM) (Figure 4A). A higher inhibitor concentration changed the kinetics closer to zero order at all [S] (Figure 4B).

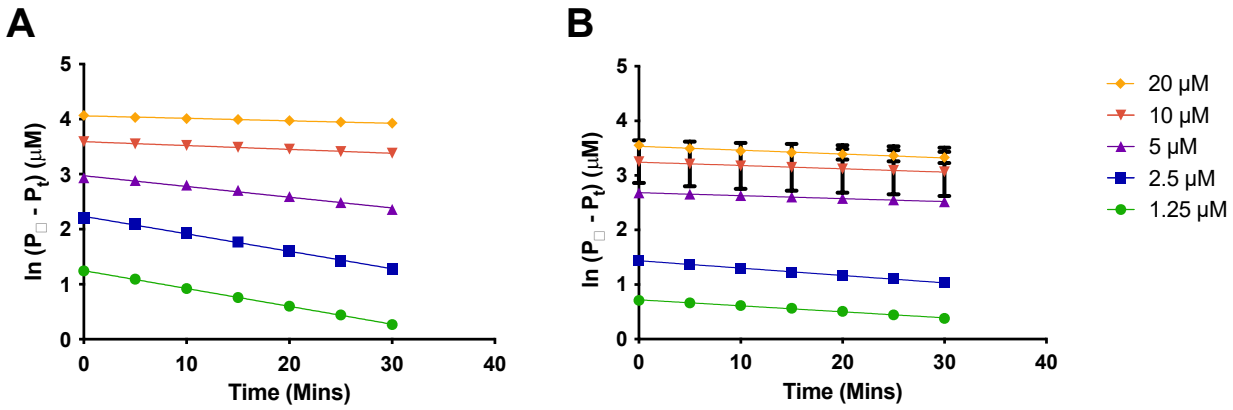

Figure 2.4. Plots of $\ln([P]_\infty - [P])$ vs. time to determine the apparent inactivation rate constant of soluble epoxide hydrolase in the presence of (A) 25 µM YMSV, and (B) 250 µM YMSV.

A plot of the apparent inactivation rate constant, A against [S] shows the protective effect a substrate may have on an enzyme. The plot derived from the $1/A$ vs. [S] showed no change in A at [S] below 5 µM, followed by a gradual increase in A as [S] increased in the absence and at low concentration (25 µM) of YMSV. However, at a high concentration of YMSV (250 µM), A increased below [S] of 5 µM, followed by a decrease in A thereafter (Figure 6). No effect on A at low [S] indicates the lack of protective effects by the substrate, thus A is independent of [S] at the lowest YMSV concentration, and to a lesser extent at 250 µM YMSV. This similarity reflects the minimal inhibition that occurred at low inhibitor concentrations. A started to increase with increasing [S], in the presence of 25 µM inhibitor, suggesting the loss of protective effects by the

substrate. At 250 µM YMSV, the opposite effect was observed where *A* increased at [S] >5 µM, suggesting protective effects of the substrate. Taken together, the concentration-dependent effects of the inhibitor on the protective effects of the substrate are apparent.

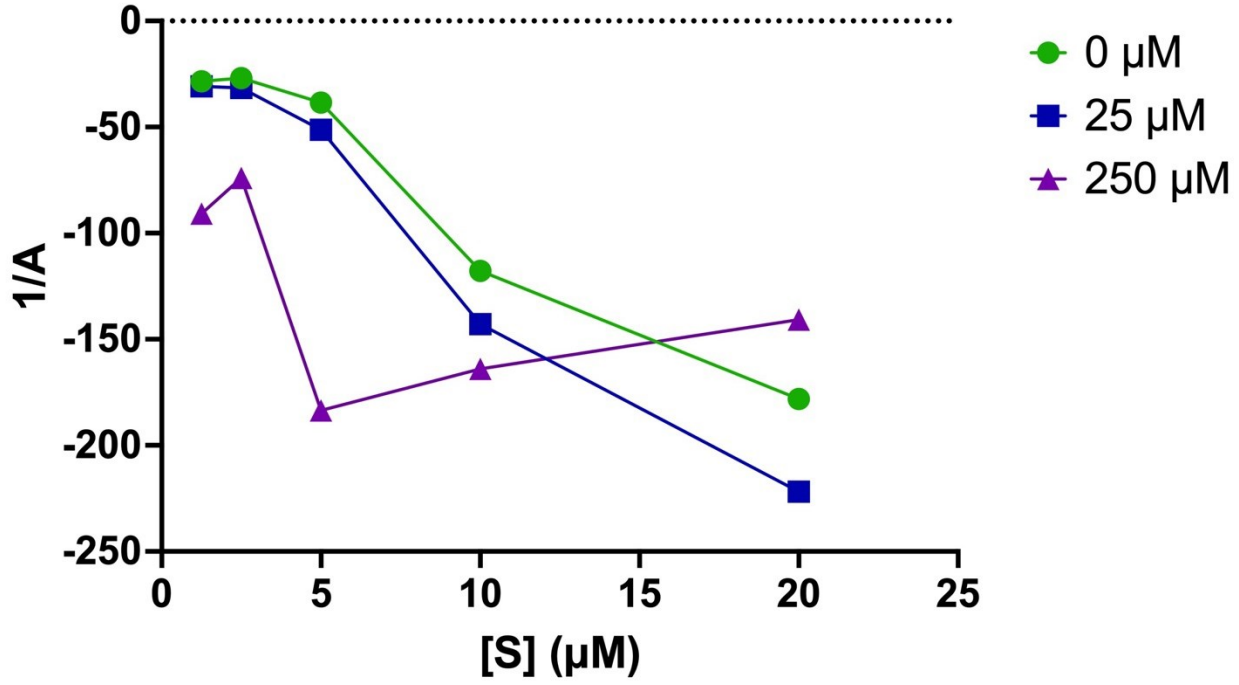

Figure 2.5. Plots of the reciprocal of apparent inactivation rate constant (*A*) vs. [S] in the absence and presence of different concentrations of inhibitor (25 and 250 µM YMSV).

2.3.4. Effect of YMSV on the secondary structure of sEH

Circular dichroism was used to evaluate the effect of YMSV on the secondary structure of sEH toward understanding the potential structural mechanism of inhibition. The pattern of CD spectra obtained for the native sEH is similar to previously reported data (Abis et al., 2019b; de Oliveira et al., 2016). The spectra of sEH control showed the appearance of an absorption maximum at ~196 nm, a broad negative band with a peak at 207 nm, and a slight shoulder at 222 nm. This absorption pattern suggests the presence of some α-helical content in the secondary structure, the appearance of a broad positive peak from 192–196 nm as well as the negative peak between 210 nm and 220 nm indicating the presence of β-sheet content. As shown in Table 1, the Bestsel program indicated the presence of 23.7% α-helix, 36.1 % anti-parallel β-sheets, 20.1 % parallel β-sheets, and 20.1% turns in sEH control. The presence of YMSV resulted in the disappearance of

the strong positive peak with a concomitant broadening of the strong negative peak ranging at 200–235 nm, with a shift in the negative peak and shoulder to 202 and 226 nm, respectively (Figure 6). Analysis with Bestsel indicated that sEH, in the presence of YMSV, contained 16% α-helix, 47.5% anti-parallel β-sheets, 14.4% turns, and 22% others. The addition of YMSV altered the secondary structure contents illustrated by the decrease in α-helical and turns contents and complete loss of parallel β-sheets, some of which may have been converted into the more stable anti-parallel β-sheets. The undefined secondary structures observed in the presence of YMSV could be random coils, suggesting that the inhibitor-induced sEH protein unfolding.

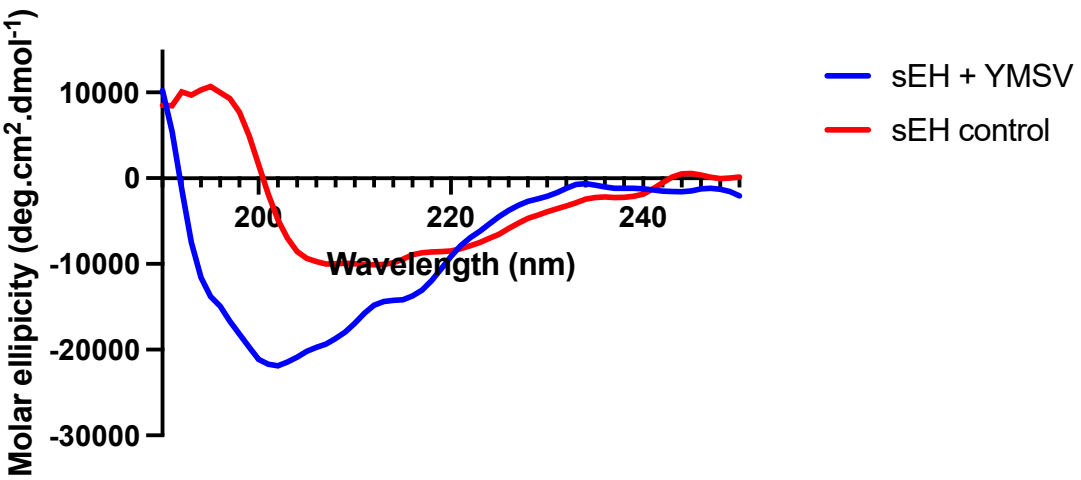

Figure 2.6. Circular dichroism spectra of soluble epoxide hydrolase in the absence (sEH control) and presence (sEH+YMSV) of the inhibitor peptide.

2.3.5. Molecular docking showing YMSV complexation with sEH

Molecular docking was used to examine the protein-ligand interaction and mechanism by which YMSV inhibited human sEH. The two molecular simulations carried out include active site and blind docking. At sEH active site, the C-terminal hydrolase pocket includes two tyrosine resides, Tyr381 and Tyr465, and a catalytic triad, Asp333-Asp495-His523, which is situated right across from the hydrolase pocket. The carboxylic acid of Asp333 forms an ester bond with the epoxide, which is an important step in epoxide hydrolysis. Due to the nucleophilic nature of Asp333, it can accept hydrogen atom from the amino group (-NH) of the inhibitor peptide to form a hydrogen bond with its oxygen atom. This is the rationale for the competitive inhibition mechanism exhibited by urea- and amide-based sEH inhibitors (Shen & Hammock, 2012). YMSV docking at the active

site showed multiple interactions with the sEH, including hydrogen bonding and π-π stacking (Figure 8A). The amino group (NH_3^+) at the N-terminal of YMSV was predicted to donate a hydrogen atom to Asp335 in the active site, which corresponds to Asp333 of the catalytic triad. The formation of this hydrogen bond (2.043 Å) confirmed that YMSV could be a competitive inhibitor for sEH. The tyrosine residue of YMSV was also able to have π-π stacking interaction with the Trp 336A. The hydroxymethyl group of Ser and the C-terminus carboxyl group of YMSV participated as ligand acceptors from Asn366A and Ser374A residues, respectively (Figure 8A). Additional interactions between YMSV and side chains (Asn378A, Asn472A, Trp473A, Tyr383A, Tyr446A, Gln384A, Ile363A, Phe381A, Tyr343A, Met339A, Leu499A and Met503A), backbone amino acids (Pro364A), and backbone side chain residues (Pro371A and Met469A) were also observed (Figure 8A). Similarly, competitive inhibition was previously reported for methyl rosmarinate, dimethyl lithospermate and 9″ methyl lithospermate, with similar interacting amino acid residues in sEH as that of AUDA (Han et al., 2021). The binding affinity of YMSV at the active site of sEH was predicted to be -7.669 $kcal.mol^{-1}$.

The blind or free docking of YMSV with sEH showed that the hydroxyl group of Tyr and the amino group at the N-terminal of YMSV acted as a ligand donor to Leu228A and Arg103A residues while the carboxyl group of the C-terminus served as a ligand acceptor for Ala284A residue (Figure 8C). YMSV also interacted with other side chains (Leu110A, Thr230A, His146A, Asn535A, Met145A, Pro229A, Pro227A, and Ile539A) and backbone side chain residues (Leu106A, Pro279A, Gln283A, Ala280A, Thr532A, and Gln107A) of human sEH (Figure 8C). The binding affinity was predicted to be -6.612 $kcal.mol^{-1}$ (Figure 8D). These findings support the inhibition kinetics results that showed mixed-competitive inhibition.

The previous study with corn gluten tripeptide WEY, a mixed-competitive inhibitor, reported a binding affinity of -10.3024 $kcal.mol^{-1}$ for the sEH active site (Dang et al., 2022), which was lower that the binding affinities of YMSV from both the active site and blind docking. This implies that YMSV has a lower binding affinity for sEH compared to tripeptides. Nonetheless, the binding affinity and number of interactions of YMSV predicted at the active site were more favorable than those obtained from blind docking. This shows that YMSV has a higher probability of binding sEH at its active site than other binding sites on the enzyme. In addition, the bond lengths of the

hydrogen bonds that were generated at the regulatory and active sites were adequate (Fakhar et al., 2022).

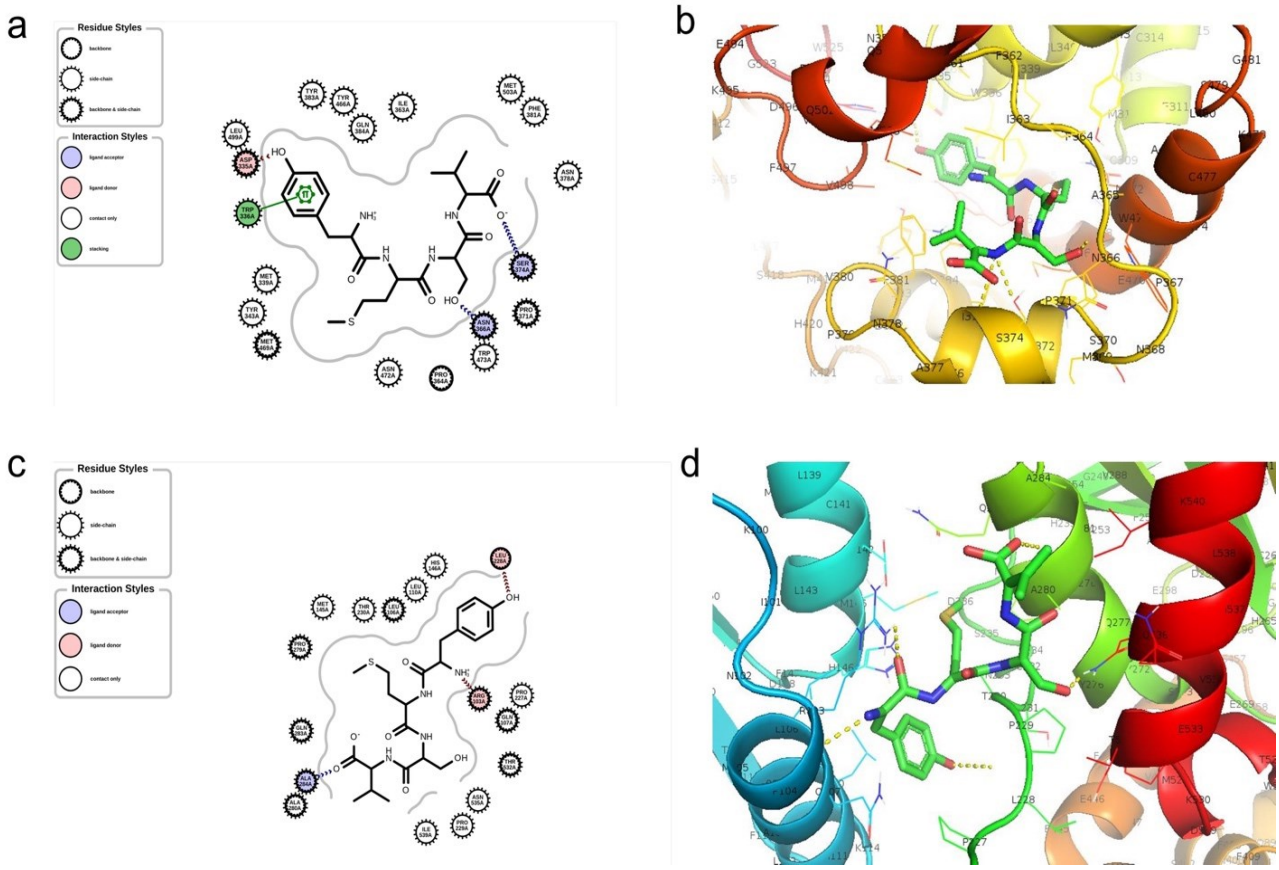

Figure 2.7. Molecular docking simulation showing (A) 2D and (B) 3D binding interaction of YMSV peptide and the active site of human soluble epoxide hydrolase (sEH), (C) 2D and (D) 3D binding interaction of YMSV peptide and human sEH upon blind docking.

2.3.6. Comparative in silico drug-likeness of the inhibitors

The computational analysis of the pharmacokinetics and drug-likeness of molecules is a cheaper, faster and non-invasive tool used to predict the behavior of molecules in biological systems (Daina et al., 2019). The SwissADME software was used to predict the ADME (absorption, distribution, metabolism, excretion, and toxicity) potential, which provides the pharmacokinetics, pharmacochemistry, drug-likeness, lipophilicity, and solubility parameters (Daina et al., 2017). The drug-likeness parameters of YMSV were compared to that of AUDA, a widely used strong sEH inhibitor. As shown in Table 2, YMSV is a larger molecule than AUDA; however, it is a small molecule with a molecular weight <500 Da, which is a prerequisite for drug-likeness (Daina et al., 2017, 2019; Ranjith and Ravikumar, 2019). Solubility and lipophilicity are crucial parameters in pharmacokinetics as they describe the interaction of molecules within aqueous and lipid environments. YMSV had a solubility scale Log S value of 0.23, indicating that it is highly soluble compared to AUDA (Log S, -4.98), which can be classified as moderately soluble. AUDA also had a higher CLogP value than YMSV, which has a negative value, indicating a higher affinity for the aqueous phase as confirmed by the ESOL prediction. Compounds having a logP higher than 1 or less than 4 are often thought to have suitable physicochemical and ADME properties required for oral drug intake (Arnott & Planey, 2012). Also, high lipophilicity is characterized by poor solubility, high metabolic rate, and poor absorption, making the compounds potentially harmful as they can accumulate in the body and become toxic (Liu et al., 2011). Most identified sEH inhibitors act by binding to the active site, but their low water solubility impedes their clinical use for the treatment of diseases related to sEH and the inflammatory pathway (Sun et al., 2021). Consequently, a few sEH inhibitors, such as 1,3-disubstituted urea and amide-based inhibitors, have been designed with improved solubility (Kim et al., 2004, 2005). Apart from solubility, these inhibitors are cumbersome in size and, even if when soluble in the bloodstream, may not be able to escape biotransformation in the gastrointestinal tract or by the liver enzymes, thereby reducing their bioavailability (Sun et al., 2021). YMSV is particularly susceptible to such modifications, hence its low GIA (Table 2). A previous study demonstrated the bioavailability of YMSV may be reduced due to its high hydrophobicity and lack of charges, which led to its weak mucin-binding properties and low mucus permeation (Sun et al., 2021). YMSV does not inhibit cytochrome P450 3A4 and is a P-glycoprotein substrate; thus, it can be rapidly metabolized and removed from cells in the body which suggests its suitability for human consumption. In addition to sEH inhibition,

YMSV was previously reported to inhibit the fibrillation of islet amyloid polypeptide, a factor that contributes to the development of type 2 diabetes (Abioye et al., 2022). Thus, YMSV has promise as a multifunctional nutraceutical compound.

Table 2.2. ***In silico*** **absorption, distribution, metabolism, and excretion (ADME) profile of YMSV peptide and AUDA generated using SwissADME.**

		YMSV	**AUDA**
Physicochemical properties	MW (g/mol)	498.59	392.58
	ROTB (n)	17	15
	HBA (n)	8	3
	HBD (n)	7	3
	ESOL (Log S)	0.23	- 4.98
Lipophilicity	TPSA ($Å^2$)	216.38	78.43
	CLogP (o/w)	-0.39	4.69
Drug-likeness and pharmacokinetics	Bioavailability score	0.17	0.56
	GIA	Low	High
	Lipinski filter	No	Yes
	P-glycoprotein substrate	Yes	No
	CYP 3A4 inhibitor	No	Yes
	BBB permeation	No	No

Abbreviations: Molecular Weight (MW) (g/mol); Number Of Rotatable Bonds (ROTB); Hydrogen Bond Donors (HBD); Hydrogen Bond Acceptors (HBA); Estimated Solubility

(ESOL) (Delaney, 2004)**; Toxin Support Vector Machine (SVM) score (BIOPEP and ToxinPred)** (Gupta et al., 2013)**; Topological Polar Surface Area (TPSA); Logarithm Of Compound Partition Coefficient Between N-Octanol And Water (ClogP); Bioavailability score, probability of F > 10% in rat** (Martin, 2005)**; Lipinski Filter (Lipinski's Rule-Of-5); Gastrointestinal Absorption (GIA); P-Glycoprotein Substrate, and Cytochrome P450 3A4 (CYP3A4) Inhibitor; Blood Brain Barrier (BBB) permeation.**

2.4. Conclusion

In this study, YMSV was identified as a new mixed-competitive inhibitor of sEH. The interaction of YMSV with sEH resulted in the loss of α-helical and β-sheet content of the enzyme, in favor of unstructured random coil conformation. Molecular docking reveals a myriad of interactions within the catalytic site and backbone residue side chains, which support the proposed mode of inhibition. Predictions of ADME indicate that some of the pharmacokinetics and drug-likeness properties of YMSV are better than AUDA, although the peptide is predicted to have low gastrointestinal absorption and oral bioavailability. Future research should include the development of processing methods to release the bioactive peptide from its parent proteins as well as *in vivo* physiological bioactivity and pharmacokinetics assessments. Taken together, this study provides important insight into the mechanism by which peptides inhibit sEH activity toward future applications as nutraceuticals for the management of inflammatory diseases.

Abbreviations

AUDA, 12-(3-adamantan-1-yl-ureido)dodecanoic acid; COX-2, cyclooxygenase-2; DHET, dihydroxyeicosatrienoic acid; EET, epoxyeicosatrienoic acid; EpFAs, epoxy-fatty acids; FAAH, fatty acid amide hydrolase; ICAM-1, intercellular adhesion molecule 1; IL-1β, interleukin-1 beta; NF-κB, nuclear factor-kappa B; Nrf2, nuclear factor erythroid 2–related factor 2; PPAR, peroxisome proliferator-activated receptor; PTUPB, 4-(5-Phenyl-3-(3-(3-(4-(trifluoromethyl)phenyl)ureido)propyl)-1H-pyrazol-1-yl)benzenesulfonamide; *t*-TUCB, trans-4-[4-(3-trifluoromethoxyphenyl-l-ureido)-cyclohexyloxy]-benzoic acid; TNF- α, tumor necrosis factor-α; VCAM-1, vascular cell adhesion molecule 1.

Funding

This research was supported by the University Research Chair Program of the University of Ottawa, and the Natural Sciences and Engineering Research Council of Canada (NSERC), RGPIN-2018-06839.

Data Availability Statement

The article contains data supporting the findings.

Acknowledgments

J.I.O. is a recipient of the University of Ottawa Nutrition and Mental Health Scholarship. R.A. is a recipient of the Vanier Canada Graduate Scholarship.

2.5. References

Abioye, R. O., Okagu, O. D., & Udenigwe, C. C. (2022). Disaggregation of Islet Amyloid Polypeptide Fibrils as a Potential Anti-Fibrillation Mechanism of Tetrapeptide TNGQ. *International Journal of Molecular Sciences*, *23*(4). https://doi.org/10.3390/ijms23041972

Abis, G., Charles, R. L., Eaton, P., & Conte, M. R. (2019). Expression, purification, and characterisation of human soluble Epoxide Hydrolase (hsEH) and of its functional C-terminal domain. *Protein Expression and Purification*, *153*. https://doi.org/10.1016/j.pep.2018.09.001

Abis, G., Charles, R. L., Kopec, J., Yue, W. W., Atkinson, R. A., Bui, T. T. T., Lynham, S., Popova, S., Sun, Y. B., Fraternali, F., Eaton, P., & Conte, M. R. (2019). 15-deoxy-Δ12,14-Prostaglandin J2 inhibits human soluble epoxide hydrolase by a dual orthosteric and allosteric mechanism. *Communications Biology*, *2*(1). https://doi.org/10.1038/s42003-019-0426-2

Arnott, J. A., & Planey, S. L. (2012). The influence of lipophilicity in drug discovery and design. In *Expert Opinion on Drug Discovery* (Vol. 7, Issue 10). https://doi.org/10.1517/17460441.2012.714363

Buscató, Estel. la, Blöcher, R., Lamers, C., Klingler, F.-M., Hahn, S., Steinhilber, D., Schubert-Zsilavecz, M., & Proschak, E. (2012). Design and Synthesis of Dual Modulators of Soluble Epoxide Hydrolase and Peroxisome Proliferator-Activated Receptors. *Journal of Medicinal Chemistry*, *55*(23), 10771–10775. https://doi.org/10.1021/jm301194c

Cuong, T. D., Anh, H. T. N., Huong, T. T., Khanh, P. N., Ha, V. T., Hung, T. M., Kim, Y. H., & Cuong, N. M. (2019). Identification of soluble epoxide hydrolase inhibitors from the seeds of passiflora edulis cultivated in Vietnam. *Natural Product Sciences*, *25*(4). https://doi.org/10.20307/nps.2019.25.4.348

Daina, A., Michielin, O., & Zoete, V. (2017). SwissADME: A free web tool to evaluate pharmacokinetics, drug-likeness and medicinal chemistry friendliness of small molecules. *Scientific Reports*, *7*. https://doi.org/10.1038/srep42717

Daina, A., Michielin, O., & Zoete, V. (2019). SwissTargetPrediction: updated data and new features for efficient prediction of protein targets of small molecules. *Nucleic Acids Research*, *47*(W1). https://doi.org/10.1093/nar/gkz382

Dang, J., Du, S., & Wang, L. (2022). Screening and Identification of Novel Soluble Epoxide Hydrolase Inhibitors from Corn Gluten Peptides. *Foods*, *11*(22), 3695. https://doi.org/10.3390/foods11223695

de Oliveira, G. S., Adriani, P. P., Borges, F. G., Lopes, A. R., Campana, P. T., & Chambergo, F. S. (2016). Epoxide hydrolase of Trichoderma reesei: Biochemical properties and conformational characterization. *International Journal of Biological Macromolecules*, *89*, 569–574. https://doi.org/10.1016/j.ijbiomac.2016.05.031

Delaney, J. S. (2004). ESOL: Estimating aqueous solubility directly from molecular structure. *Journal of Chemical Information and Computer Sciences*, *44*(3). https://doi.org/10.1021/ci034243x

Eberhardt, J., Santos-Martins, D., Tillack, A. F., & Forli, S. (2021). AutoDock Vina 1.2.0: New Docking Methods, Expanded Force Field, and Python Bindings. *Journal of Chemical Information and Modeling*, *61*(8). https://doi.org/10.1021/acs.jcim.1c00203

Fakhar, Z., Hejazi, L., Tabatabai, S. A., & Munro, O. Q. (2022). Discovery of novel heterocyclic amide-based inhibitors: an integrative in-silico approach to targeting soluble epoxide hydrolase. *Journal of Biomolecular Structure and Dynamics*, *40*(15). https://doi.org/10.1080/07391102.2021.1894987

Guha, S., & Majumder, K. (2019). Structural-features of food-derived bioactive peptides with anti-inflammatory activity: A brief review. *Journal of Food Biochemistry*, *43*(1), e12531-n/a. https://doi.org/10.1111/jfbc.12531

Gupta, S., Kapoor, P., Chaudhary, K., Gautam, A., Kumar, R., & Raghava, G. P. S. (2013). In Silico Approach for Predicting Toxicity of Peptides and Proteins. *PLoS ONE*, *8*(9). https://doi.org/10.1371/journal.pone.0073957

Han, Y. K., Lee, J. S., Yang, S. Y., Lee, K. Y., & Kim, Y. H. (2021). In vitro and in silico studies of soluble epoxide hydrolase inhibitors from the roots of lycopus lucidus. *Plants*, *10*(2). https://doi.org/10.3390/plants10020356

Hollinshead, M., & Meijer, J. (1988). Immunocytochemical analysis of soluble epoxide hydrolase and catalase in mouse and rat hepatocytes demonstrates a peroxisomal localization before and after clofibrate treatment. *European Journal of Cell Biology*, *46*(3).

Hwang, S. H., Wagner, K. M., Morisseau, C., Liu, J. Y., Dong, H., Wecksler, A. T., & Hammock, B. D. (2011). Synthesis and structure-activity relationship studies of urea-containing

pyrazoles as dual inhibitors of cyclooxygenase-2 and soluble epoxide hydrolase. *Journal of Medicinal Chemistry*, *54*(8). https://doi.org/10.1021/jm2001376

Iyer, M. R., Kundu, B., & Wood, C. M. (2022). Soluble epoxide hydrolase inhibitors: an overview and patent review from the last decade. *Expert Opinion on Therapeutic Patents*, *32*(6), 629–647. https://doi.org/10.1080/13543776.2022.2054329

Jo, A. R., Kim, J. H., Yan, X. T., Yang, S. Y., & Kim, Y. H. (2016). Soluble epoxide hydrolase inhibitory components from Rheum undulatum and in silico approach. *Journal of Enzyme Inhibition and Medicinal Chemistry*, *31*. https://doi.org/10.1080/14756366.2016.1189421

Khan, H. A. Md., Liu, J., Kumar, G., Skapek, S. X., Falck, J. R., Imig, J. D., -Khan, A. H., Liu, J., Kumar, G., & Skapek, S. X. (2013). Novel orally active epoxyeicosatrienoic acid (EET) analogs attenuate cisplatin nephrotoxicity; Novel orally active epoxyeicosatrienoic acid (EET) analogs attenuate cisplatin nephrotoxicity. *The FASEB Journal • Research Communication*, *27*(8), 2946–2956. https://doi.org/10.1096/fj.12-218040

Kim, I. H., Heirtzler, F. R., Morisseau, C., Nishi, K., Tsai, H. J., & Hammock, B. D. (2005). Optimization of amide-based inhibitors of soluble epoxide hydrolase with improved water solubility. *Journal of Medicinal Chemistry*, *48*(10). https://doi.org/10.1021/jm0500929

Kim, I. H., Morisseau, C., Watanabe, T., & Hammock, B. D. (2004). Design, Synthesis, and Biological Activity of 1,3-Disubstituted Ureas as Potent Inhibitors of the Soluble Epoxide Hydrolase of Increased Water Solubility. *Journal of Medicinal Chemistry*, *47*(8). https://doi.org/10.1021/jm030514j

Kim, J. H., Jo, Y. D., & Jin, C. H. (2019). Isolation of soluble epoxide hydrolase inhibitor of capsaicin analogs from Capsicum chinense Jacq. cv. Habanero. *International Journal of Biological Macromolecules*, *135*. https://doi.org/10.1016/j.ijbiomac.2019.06.028

Kodani, S. D., Bhakta, S., Hwang, S. H., Pakhomova, S., Newcomer, M. E., Morisseau, C., & Hammock, B. D. (2018). Identification and optimization of soluble epoxide hydrolase inhibitors with dual potency towards fatty acid amide hydrolase. *Bioorganic and Medicinal Chemistry Letters*, *28*(4). https://doi.org/10.1016/j.bmcl.2018.01.003

Lee, K. S. S., Ng, J. C., Yang, J., Hwang, S. H., Morisseau, C., Wagner, K., & Hammock, B. D. (2020). Preparation and evaluation of soluble epoxide hydrolase inhibitors with improved physical properties and potencies for treating diabetic neuropathic pain. *Bioorganic and Medicinal Chemistry*, *28*(22). https://doi.org/10.1016/j.bmc.2020.115735

Liu, X., Testa, B., & Fahr, A. (2011). Lipophilicity and its relationship with passive drug permeation. In *Pharmaceutical Research* (Vol. 28, Issue 5). https://doi.org/10.1007/s11095-010-0303-7

Martin, Y. C. (2005). A bioavailability score. *Journal of Medicinal Chemistry*, *48*(9). https://doi.org/10.1021/jm0492002

Micsonai, A., Wien, F., Bulyáki, É., Kun, J., Moussong, É., Lee, Y. H., Goto, Y., Réfrégiers, M., & Kardos, J. (2018). BeStSel: A web server for accurate protein secondary structure prediction and fold recognition from the circular dichroism spectra. *Nucleic Acids Research*, *46*(W1). https://doi.org/10.1093/nar/gky497

Miles, A. J., & Wallace, B. A. (2018). CDtoolX, a downloadable software package for processing and analyses of circular dichroism spectroscopic data. *Protein Science*, *27*(9). https://doi.org/10.1002/pro.3474

Morisseau, C., & Hammock, B. D. (2013). Impact of soluble epoxide hydrolase and epoxyeicosanoids on human health. In *Annual Review of Pharmacology and Toxicology* (Vol. 53). https://doi.org/10.1146/annurev-pharmtox-011112-140244

Morris, G. M., Ruth, H., Lindstrom, W., Sanner, M. F., Belew, R. K., Goodsell, D. S., & Olson, A. J. (2009). Software news and updates AutoDock4 and AutoDockTools4: Automated docking with selective receptor flexibility. *Journal of Computational Chemistry*, *30*(16). https://doi.org/10.1002/jcc.21256

Ranjith D and Ravikumar C. (2019). SwissADME predictions of pharmacokinetics and drug-likeness properties of small molecules present in Ipomoea mauritiana Jacq. *Journal of Pharmacognosy and Phytochemistry*, *8*(5).

Rentzsch, R., & Renard, B. Y. (2015). Docking small peptides remains a great challenge: An assessment using AutoDock Vina. *Briefings in Bioinformatics*, *16*(6). https://doi.org/10.1093/bib/bbv008

Scheiner, S., Kar, T., & Pattanayak, J. (2002). Comparison of various types of hydrogen bonds involving aromatic amino acids. *Journal of the American Chemical Society*, *124*(44). https://doi.org/10.1021/ja027200q

Schiøtt, B., & Bruice, T. C. (2002). Reaction mechanism of soluble epoxide hydrolase: Insights from molecular dynamics simulations. *Journal of the American Chemical Society*, *124*(49). https://doi.org/10.1021/ja021021r

Shen, H. C., & Hammock, B. D. (2012). Discovery of inhibitors of soluble epoxide hydrolase: A target with multiple potential therapeutic indications. In *Journal of Medicinal Chemistry* (Vol. 55, Issue 5). https://doi.org/10.1021/jm201468j

Sun, C.P., Zhang, X.Y., Morisseau, C., Hwang, S. H., Zhang, Z.-J., Hammock, B. D., & Ma, X.C. (2021). Discovery of Soluble Epoxide Hydrolase Inhibitors from Chemical Synthesis and Natural Products. *Journal of Medicinal Chemistry*, *64*(1), 184–215. https://doi.org/10.1021/acs.jmedchem.0c01507

Sun, X., Abioye, R. O., Okagu, O. D., & Udenigwe, C. C. (2021). Peptide-Mucin Binding and Biosimilar Mucus-Permeating Properties. *Gels*, *8*(1), 1. https://doi.org/10.3390/gels8010001

Swardfager, W., Hennebelle, M., Yu, D., Hammock, B. D., Levitt, A. J., Hashimoto, K., & Taha, A. Y. (2018). Metabolic/inflammatory/vascular comorbidity in psychiatric disorders; soluble

epoxide hydrolase (sEH) as a possible new target. *Neuroscience and Biobehavioral Reviews*, *87*, 56–66. https://doi.org/10.1016/J.NEUBIOREV.2018.01.010

Tao, A., Huang, Y., Shinohara, Y., Caylor, M. L., Pashikanti, S., & Xu, D. (2019). EzCADD: A Rapid 2D/3D Visualization-Enabled Web Modeling Environment for Democratizing Computer-Aided Drug Design. *Journal of Chemical Information and Modeling*, *59*(1). https://doi.org/10.1021/acs.jcim.8b00633

Tonolo, F., Folda, A., Scalcon, V., Marin, O., Bindoli, A., & Rigobello, M. P. (2022). Nrf2-Activating Bioactive Peptides Exert Anti-Inflammatory Activity through Inhibition of the NF-κB Pathway [Article]. *International Journal of Molecular Sciences*, *23*(8), 4382. https://doi.org/10.3390/ijms23084382

Trott, O., & Olson, A. J. (2010). AutoDock Vina: Improving the speed and accuracy of docking with a new scoring function, efficient optimization, and multithreading. *Journal of Computational Chemistry*. https://doi.org/10.1002/jcc.21334

Udenigwe, C. C., Abioye, R. O., Okagu, I. U., & Obeme-Nmom, J. I. (2021). Bioaccessibility of bioactive peptides: recent advances and perspectives [Article]. *Current Opinion in Food Science*, *39*, 182–189. https://doi.org/10.1016/j.cofs.2021.03.005

Zhang, G., Panigrahy, D., Hwang, S. H., Yang, J., Mahakian, L. M., Wettersten, H. I., Liu, J. Y., Wang, Y., Ingham, E. S., Tam, S., Kieran, M. W., Weiss, R. H., Ferrara, K. W., & Hammock, B. D. (2014). Dual inhibition of cyclooxygenase-2 and soluble epoxide hydrolase synergistically suppresses primary tumor growth and metastasis. *Proceedings of the National Academy of Sciences of the United States of America*, *111*(30). https://doi.org/10.1073/pnas.1410432111

CHAPTER 3 – QUANTITATIVE STRUCTURE-ACTIVITY RELATIONSHIP MODELLING OF TRIPEPTIDE INHIBITORS OF THE HUMAN SOLUBLE EPOXIDE HYDROLASE ENZYME

Abstract

The use of food peptides as nutraceuticals has increased in the pharmaceutical industry due to the low cost of production and robust bioactivities coupled with little or no side effects because they are dietary, to begin with. Previously, tripeptides from corn gluten were analyzed for their inhibitory action against soluble epoxide hydrolase (sEH), however, the relationship between the amino acid constituents of the peptides structure and inhibitory activity is yet to be understood. sEH inhibitory tripeptides validated in the literature were used as the primary dataset after which they were analyzed using the two-terminal positional numbering method, and quantitative structural activity relationship (QSAR) modelling was performed on the peptide list using SIMCA® software. The FASGAI and VHSE descriptors were selected for PLS regression of the dataset, however, the FASGAI model performed better. The models were generated using partial least square (PLS) regression and validated by cross-validation and permutation tests (R^2 = 0.33 and Q^2 = 0.09). The positions of amino acid residues in the tripeptide sequence were ranked according to importance as n1>n3>n2 with the top-scoring properties being electronic/charge, hydrophobic, and bulk/size properties. Our findings show that nonpolar, hydrophobic, bulky amino acids such as Trp, Tyr, and Phe are preferred at the N-terminus end and since these amino acids are also considered to be rigid, having low alpha and turn propensities, they are also preferred at the C-terminus end of the tripeptide for optimum inhibition of sEH. The models were further used to predict the inhibitory activity of a test set comprising 9 bioactive tripeptides but did not exhibit satisfactory performance. The insights drawn from this dataset could be nongeneralizable due to the invariability of the data, however, this provides information on the characteristics of the inhibitory tripeptides and contributes to the ongoing research on food peptide and small molecule inhibitors of soluble epoxide hydrolase.

Keywords: Soluble epoxide hydrolase (sEH), quantitative structure-activity relationship (QSAR), tripeptide, sEH inhibition, amino acid properties, FASGAI

3.1. Introduction

The soluble epoxide hydrolase enzyme (sEH) is associated with the human inflammatory system, making it a suitable molecular target to explore therapeutic options for the treatment and management of cardiovascular diseases such as high BP and heart failure, gastrointestinal disorders like inflammatory bowel disease and mental conditions like depression (Wagner et al., 2017). This enzyme functions by metabolizing Epoxyeicosatrienoic acids (EET), an epoxy fatty acid (EpFA) integral to the anti-inflammatory function of the body into less biologically active DHETs. Accordingly, the inhibitors of sEH have been vastly studied and categorized into synthetic and natural inhibitors, recognizing their various pharmacological properties (Sun et al., 2021). sEH inhibitors (sEHIs) were used as therapeutics for neuropathic and inflammatory pain treatment by reducing endoplasmic reticulum (ER) stress in diabetic rats and ameliorating severe laminitis in horses (Guedes et al., 2017; Inceoglu et al., 2015). Some inhibitors are said to have more potency than traditional NSAIDs in pain reduction and serve as dual inhibitors for the COS and LOX pathway to reduce inflammatory pain (Wagner et al., 2017). The antihypertensive effect of sEHIs is another reason for targeting sEH; the regulation of vasodilation, reduction of blood pressure and increase in sodium excretion by elevated levels of EETs by inhibiting the MAPK and NF-κB signaling pathway, thereby resulting in a decrease in the progression of cardiovascular diseases thereby contributing to the improvement of a major public concern (Luo et al., 2021). Natural inhibitors such as N-Benzyl-linoleamide, found in *Lepidium meyenii* Walp. *(L. meyenii)* are orally bioavailable in murine models and serve as excellent anti-inflammatory remedies for inflammatory pain (Singh et al., 2020). Apart from in vitro and in vivo determination of sEH inhibition, drug candidates have been tested for clinical use; AR9281 to target hypertension and type 2 diabetes (Chen et al., 2012), GSK2256294 for treatment of Chronic obstructive pulmonary disease, or COPD in obese smokers (Lazaar et al., 2016), and EC5026 to manage neuropathic pain (Hammock et al., 2021). However, due to poor pharmacokinetic properties such as low oral bioavailability and absorption as well as poor metabolism, sEHIs have not been made clinically available for the treatment and improvement of health conditions. This has directed attention to the discovery of novel sEH inhibitors including food-derived bioactive peptides. Recent studies have shown that food-derived peptides and enzyme hydrolysates have inhibitory actions against sEH activity in vitro (Dang et al., 2022; Obeme-Nmom et al., 2023). Identification of effective food-based inhibitors of sEH can initiate the development of functional foods which will be cheaper and have

zero side effects. Furthermore, identifying key pharmacophoric structural properties of these food peptides that play crucial roles in the selective inhibition of SEH can initiate the design and synthesis of more efficient inhibitors of sEH with anti-inflammatory, antihypertensive, and analgesic properties. Unfortunately, there are few or no studies on the structural requirements for food peptide inhibitors of sEH strictly consisting of amino acids.

Quantitative Structure-Activity Relationship (QSAR) is a computational modelling approach used in drug discovery, environmental science, and other fields to predict the biological activity or properties of a molecule based on its chemical structure. QSAR models assume that there is a relationship between the structural features of a molecule and its biological activity, and this relationship can be quantified mathematically (Pathak et al., 2023). The main goal of QSAR is to develop predictive models that can estimate the activity of a compound before it is synthesized or tested in the laboratory. These models are trained using a set of compounds with known activities, where the chemical structures and corresponding activities are collected. The models then analyze the structural features of the molecules to identify patterns and correlations with the observed activities (Ganguly et al., 2021). Peptide QSAR modelling has been successfully used in the study of antimicrobial, anti-oxidative and bitter-tasting peptides as well as α-glucosidase, renin, and angiotensin-I-converting enzyme inhibition (Li & Li, 2013; Mollica et al., 2019; Udenigwe et al., 2012). QSAR studies of soluble epoxide hydrolase (sEH) inhibitors have been conducted to explore the structure-activity relationships of compounds targeting this enzyme including 3-D QSAR analysis of inhibition of murine soluble epoxide hydrolase (MsEH) by analogues of benzoylureas and arylureas, the inhibitory study of 1-Aryl-3-(1-acylpiperidin-4-yl) urea, QSAR models for classification of murine and human sEH and more recently; identification of the role of hydrophobicity in the molecular structure of existing sEH inhibitors have also been reported (Nakagawa et al., 2000; Nazari et al., 2022; Rose et al., 2010; Vázquez et al., 2023).

We want to achieve an in-depth understanding of the composition of the tripeptides and their ability to inhibit sEH for further directions on the discovery of potent peptide inhibitors of the enzyme that can be cheaper, safer, and more effective. Therefore, the objective of the study was to evaluate the contributions of individual amino acid residues based on their physicochemical and structural properties as well as the sequence and positions of the amino acids in the peptide chain

of tripeptides to inhibition of the functionally robust soluble epoxide hydrolase using quantitative structure-activity relationship (QSAR) analysis.

3.2. Materials and methods

3.2.1. Materials

sEH (Human soluble epoxide hydrolase), PHOME (3-phenyl-cyano(6-methoxy-2-naphthalenyl) methyl ester-2-oxirane acetic acid) and AUDA (12-[[(tricyclo[3.3.1.13,7]dec-1-ylamino)carbonyl]amino]-dodecanoic acid) were purchased from Cayman Chemical (Ann Arbor, Michigan, USA). Tripeptides were synthesized with a purity of over 95% by GenScript Inc. (New Jersey, USA). Bovine serum albumin (BSA), bis-Tris-HCl, 6-methoxy-2-naphthaldehyde (6M2N), and dimethyl sulfoxide (DMSO) were purchased from MilliporeSigma (Oakville, ON, Canada). All the chemical reagents are analytical grade and used without further purification.

3.2.2. Peptide synthesis/Peptide dataset

The peptide dataset is made up of 20 tripeptides obtained from corn gluten as identified by (Dang et al., 2022) (Table 1). However, external validation of the PLS model was also performed using 9 tripeptides which were derived from yellow pea protein by enzymatic hydrolysis and high-performance liquid chromatography (HPLC) fractionation and was subsequently identified via tandem mass spectrometry as previously described (Asen et al., 2022).

3.2.3. sEH Inhibition Assay

The inhibitory activity percentage of 9 tripeptides was performed as previously described by Dang et. al (Dang et al., 2022). Briefly, 130 µL of 62.5 ng/mL human sEH solution (final concentrations, dissolved in 25 mM bis-Tris-HCl containing 0.1% BSA, pH 7.0) and 20 µL of 100 µM peptides were combined in a black 96-well plate with 50 µL of 10 µM PHOME. The reaction was incubated at 37 °C and the intensity of its fluorescence was read for 40 mins at 5 mins intervals, using the Spark multimode microplate reader (Tecan, Stockholm, Sweden), at an excitation wavelength of 330 nm and emission wavelength of 460 nm. AUDA was used as the positive control and bis-Tris-HCl buffer was used as the blank control for the experiment. The inhibitory activity of sEH was calculated using the equation:

$$\%\ Inhibitory\ activity = \left(\frac{C_{40} - S_{40}}{C_{40} - S_0}\right) \times\ 100\%$$

Where the fluorescence intensity of the control reaction of sEH alone at 0 and 40 mins is C_0 and C_{40} respectively while S_{40} is the fluorescence intensity of sEH in the presence of 100 μM each peptide.

3.2.4. X-matrix

The *X*-matrix contained information for each of the 29 tripeptides. The amino acid descriptor matrix was analyzed and modelled using SIMCA® version 17.0.2 (Sartorius Stedim Data Analytics AB, Germany) based on tripeptides among 16 descriptors; FASGAI (Liang et al., 2009; Liang & Li, 2007), VHSE (Mei et al., 2004), HSEH (Shu et al., 2009), Kidera factors (Kidera et al., 1985), PPP (Sneath, 1966), ST scale (Yang et al., 2010), VTSA (Li et al., 2008), Z3 and Z5 scales (Hellberg et al., 1987), DPPS (Tian et al., 2009), T scale (Tian et al., 2007), VSTV (Mei et al., 2004), ECI and ISA (Collantes & Dunn, 1995), SVG (Tong et al., 2008),and SZOTT (Liang et al., 2008).

3.2.5. Y-matrix

The *Y*-matrix represents the % inhibition of sEH by 100 M of each peptide. In order to estimate the degree of inhibition of the peptides on soluble epoxide hydrolase, the percent inhibition of the extra 9 peptides was computed using the established % sEH inhibitory activity of 20 tripeptides by Dang et al. Thus, (*Y*) best describes the peptides' inhibitory effect on sEH.

3.2.6.PLS regression modelling

Modelling of inhibitory activity (*Y*) as a function of the amino acid descriptor (*X*) of the peptides was calculated by the partial least squared (PLS) regression using SIMCA® version 17.0.2 (Sartorius Stedim Data Analytics AB, Germany). The PLS model was statistically validated with internal validation, and outlier exclusion using Hotelling's T^2, and no external validation was performed. The multiple correlation coefficient (R^2) and the cross-validation correlation coefficient (Q^2_{cv}) were calculated using SIMCA software and used to express the model quality and predictive power, respectively. The software also computed the relative contribution of the amino acid (*X*) descriptors to the inhibitory activities of the peptides and indicated them as Variable Importance for the Projection (VIP) and coefficient plots.

3.2.7. Statistical analysis

Statistical analysis was performed using one-way analysis of variance with GraphPad Prism version 9.5.1 for Windows (GraphPad Software, La Jolla, CA, USA). The significant difference between the mean values was defined at $p < 0.05$ using Dunnett's multiple comparisons tests.

3.3. Results and Discussion

3.3.1. QSAR modelling of sEH-inhibitory tripeptides.

The evolution of the field of biologically active peptides over the years has made it an important aspect of pharmaceutical remedies for various health challenges including hypertension, cancer, diabetes, and other chronic diseases because they possess anti-inflammatory, antioxidative, immunomodulatory, cholesterol-lowering, anti-hypertensive, antimicrobial, neuroprotective effects, with many more properties yet to be explored (Chakrabarti et al., 2018). Food peptides of various lengths have been identified from plants, animals, and marine sources, however, the process of manufacturing and identification of the activities of these peptides can be tedious, time-consuming and may end up having minute or no activity. Therefore, the use of in silico methods such as Quantitative structure-activity relationship (QSAR) modelling can be used to predict the sequences and activities of bioactive peptides to overcome the challenges mentioned previously (Gu et al., 2011). QSAR modelling is a technique used in drug discovery to find novel small molecules that can bind to a protein target. The use of data from the literature is a common approach in QSAR analysis. There is validity that food-derived tripeptides and other tripeptides resulting from intestinal digestion are easily absorbed into the blood and have high biological activity (Daliri et al., 2017), this informed our selection of tripeptides for this study to generate a strong model for inhibitory tripeptides, predict the activity of other tripeptides and determine important amino acids with specific physicochemical properties that bind to the enzyme to propagate inhibition. The corn-gluten hydrolysate fraction that was utilized to identify the sEH-inhibitory tripeptides that were subsequently employed in the dataset indicated that the individual peptides had a wide range of sEH inhibitory activity (Table 3.1.).

The 15 2D and 3D descriptors used in this study served as the *X*-variables and are presented in Table 2, which shows a summary of the PLS regression results. The percent inhibition (%) of the corn tripeptides represented the *Y*-variables. The QSAR models were used to establish the

relationship between the *X* and *Y* variables and to further predict the activity of random tripeptides. The two parameters which are important in confirming the accuracy or fit of a model are (i) the coefficient of determination (R^2) and (ii) the coefficient of cross-validation (Q^2). The R^2 shows how well the data fits the models and the relationship between the observed and calculated activities whereas (Q^2) indicates the quality of the prediction of new data by the model (Li & Li, 2013). Using the 16 descriptors, the value of R^2 ranged from 0.234 to 1 and that of Q^2 ranged from -1.52 to 0.0852. Nonetheless, only 8 of the 16 descriptors showed significance for the tripeptide list and these models were further analyzed to understand the relevance of the chemical structure of the tripeptides to their inhibitory activity. The modelling of the FASGAI amino acid descriptors with *Y* resulted in a one-component PLS model that explained 33.3% of the sum of squares in *Y*-variance, the lowest of the significant models with a predictive ability of 8.52% (derived from the coefficient of cross-validation Q^2), whereas the ST scale was able to provide a sixteen-component model that could explain 97.3% of *Y* but had very low and negligible predictive power. It is also important to state that although the DPPS model was not significant, it had a positive predictive power of 0.6%, however, it is still considered to be very weak. The R^2 and Q^2 vary differently with the increase in model complexity or the number of principal components. R^2 increases as model complexity increases, however, this is not true for Q^2 as a high R^2 does not necessarily indicate a high Q^2 and this explains the very low values of Q^2 we see in the study. Therefore, the robustness of the model should be treated with caution, and this may be attributed to the reduced variety of amino acid representatives in the tripeptide list as we see that most of them consist of Tryptophan (W) and/or Tyrosine (Y) which are predominantly hydrophobic amino acids.

In QSAR analysis of a larger dataset, part of the dataset is used as a training set to establish the model while the remaining dataset serves as validated sets for external cross-validation of the predictive power of the model. In this study, the validation of the PLS models was done during modelling and a permutation test was carried out to validate the predictive capacities of the significant models. The intercepts of R^2_{cum} and Q^2_{cum} are used to measure the fit of a model with a valid model having the intercept of R^2_{cum} being < 0.3 and that of $Q^2_{cum} < 0.05$. The values observed for both parameters of the FASGAI model are in accordance with the suggested range, unfortunately, the validity of other significant models was not established.

Table 3.1. Tripeptide dataset with in vitro sEH inhibitory activity at 100 μM peptide concentration.

No.	Peptide	Inhibitory activity (%)
1.	KII	37.99 ± 8.23
2.	WKW	31.13 ± 1.24
3.	WQW	37.19 ± 6.14
4.	WRW	38.30 ± 3.66
5.	WLR	43.82 ± 1.73
6.	YRW	47.58 ± 6.23
7.	RWI	19.63 ± 10.26
8.	FKW	36.29 ± 10.08
9.	YMW	49.96 ± 5.86
10.	WYW	60.30 ± 5.60
11.	FRY	45.83 ± 14.14
12.	WWY	55.15 ± 2.38
13.	YFW	57.38 ± 7.62
14.	YHW	32.06 ± 3.06
15.	YFY	52.96 ± 3.09
16.	WTR	26.05 ± 9.78
17.	RYW	35.89 ± 2.83
18.	YHY	41.43 ± 4.19
19.	WEY	70.01 ± 6.25
20.	WFW	36.24 ± 3.73

Table 3.2. Summary of significant descriptors of the PLS modelling for the tripeptide lists of soluble epoxide hydrolase inhibitors.

No.	Model ID	A	R^2X (cum)	R^2Y (cum)	Q^2 (cum)	S/NS	Permutation Test	
							Int. R^2_{cum}	Int. Q^2_{cv}
1.	FASGAI	1	0.327	0.333	0.0852	S	0.291	-0.0557
2.	VHSE	8	0.96	0.928	-0.302	S	0.95	-2.32
3.	HSEH	9	0.915	0.954	-0.624	S	0.979	-2.76
4.	Kidera factors	16	1	0.968	-0.561	S	0.858	-2.17
5.	PPP	11	1	0.721	-0.54	S	0.63	-1.21
6.	ST scale	16	1	0.973	-1.04	S	0.963	-2.97
7.	VTSA	7	0.928	0.789	-0.148	S	0.797	-2.56
8.	z5 scale	14	1	0.885	-1.52	S	0.624	-0.864
9.	z3 scale	1	0.311	0.183	-0.1	NS	n/a	n/a
10.	DPPS	12	0.998	0.957	0.00565	NS	n/a	n/a
11.	T scale	1	0.258	0.278	-0.0796	NS	n/a	n/a
12.	VSTV	1	0.422	0.178	-0.0317	NS	n/a	n/a
13.	ECI	1	0.234	0.109	-0.1	NS	n/a	n/a
14.	ISA	1	0.344	0.114	-0.1	NS	n/a	n/a
15.	SVG	1	0.24	0.339	-0.003	NS	n/a	n/a
16.	SZOTT	1	0.125	0.568	-0.0854	NS	n/a	n/a

Abbreviations: A, number of components used for PLS analysis; R^2X, *X*-variables (descriptors) in the validated PLS models; R^2Y, multiple correlation coefficients which estimates the model fit; Q^2, cross validation correlation coefficients which evaluates the model's predictive

capabilities; Permutation test, R^2_{cum} and Q^2_{cv} were calculated by SIMCA software during model validation.

3.3.2. Prediction of sEH-inhibitory activity

Structural analysis and interpretation of descriptors of FASGAI and VHSE Scales were carried out in the present study because their physicochemical parameters are considered interpretable (Li & Li, 2013).

3.3.2.1 FASGAI

FASGAI vectors (Factor Analysis Scales of Generalized Amino Acid Information) have previously been used to describe the structure-function relationship of antimicrobial peptides and these findings show the descriptors have a clear interpretation of physicochemical parameters, can be easily modified, and manipulated, have excellent characterization capacity, and have rich structural information. The variables of FASGAI represent the hydrophobic, bulk, electrical properties, compositional characteristics, local flexibility, alpha and turn propensities, which can be used in describing the structural features of peptides and protein motifs (Liang et al., 2009; Liang & Li, 2007).

The variable importance in projection (VIP) is the sum of the variable influence overall model dimensions and is a measure of variable importance. Higher VIP values indicate a good correlation between the variable and the data. In this work, a variable is considered important when its VIP value is ≥ 1. Eight variables have relatively larger VIP values, including n3F2, n3F5, n1F6, n1F3, n3F3, n1F5, n1F2, and n1F1. These variables are particular to the amino acids in positions n1 and n3, indicating that the amino acid residues in these two positions are closely correlated with the inhibition of sEH.

According to the coefficients of the PLS model, we can evaluate the contribution of various properties of each amino acid residue to the inhibitory activity of the tripeptide and investigate the key interactions between the tripeptide and the binding site of sEH. The coefficient plot of the FASGAI model (Fig. 1) shows that n1F1, n1F3, n2F2, n2F3, n2F4, n2F5, n3F1, and n3F3 are positively correlated to *Y*, whereas n1F2, n1F4, n1F5, n1F6, n2F1, n2F6, n3F2, n3F4, n3F5and n3F6 are negatively correlated to the inhibitory activity of tripeptides.

However, based on the coefficient and VIP plots of the FASGAI model, we observed that the alpha and turn propensities of n3 were ranked the most important variable. It had a large negative correlation coefficient with sEH inhibition, this pattern was also observed for the n1 position, indicating that at the N- and C-terminals, low alpha and turn propensities are required to increase the potency of the tripeptide. The alpha and turn propensities represent the inclination of an amino acid to behave like an alpha helix or beta sheet because of the conformation of their side chains (Beck et al., 2008).

The degree of flexibility of an amino acid of the tripeptide within the active site of the enzyme could be a factor that can affect its potency and the environment, and surrounding residues, as well as the peptide structure, may affect an amino acid's local flexibility (Bhalla et al., 2006). The second important variable is the local flexibility of n3 which is negatively correlated to inhibition and this pattern is also observed at position n1 implying that at these positions, less flexible amino acids at these positions. Within the structure of a protein, amino acids can change their shape or be flexible to different degrees. This concept is known as "local flexibility". Studies have been able to categorize amino acids into high flexibility (G, E, S, K, P), intermediate flexibility (T, N, Q, D), low flexibility (W, Y, F, H, C) (Clark et al., 2019; Smith et al., 2003). This suggests that at positions 1 and 3, the rigid amino acids such as W>Y> F>H>C will be preferred in that order, moreover, the contribution of local flexibility at n3 is ranked more important than n1 (Fig. 3.1).

The electronic properties of n1 were also found to be important, however, it was negatively correlated with *Y*. Therefore, the amino acids at the N-terminus should be non-polar for increased activity. Additionally, the hydrophobicity index of n1 was also classified as important and positively correlated with *Y*, this means that the more hydrophobic that amino acid at n1 is, the more potent the tripeptide will be at sEH inhibition.

In addition, we see those bulky amino acids at the N- and C-terminals of a tripeptide could increase its sEH inhibitory property. Although the bulkiness of n2 contributes less than that of n1 and n3, this variable is not ranked important for inhibition. Consequently, we can speculate that a tripeptide that high bulk properties would efficiently inhibit sEH.

Table 3.3. Summary of important peptide properties and their positions after PLS analysis using FASGAI Vectors.

Variable	Position	Properties	VIP value	Regression Coefficient
n3F2	3	Alpha and turn propensities	1.98305	-0.121567
n3F5	3	Local flexibility	1.59063	-0.0975103
n1F6	1	Electronic	1.28254	-0.0786232
n1F3	1	Bulk	1.22609	0.0751627
n3F3	3	Bulk	1.22177	0.0748976
n1F5	1	Local flexibility	1.20267	-0.073727
n1F2	1	Alpha and turn propensities	1.08861	-0.0667346
n1F1	1	Hydrophobicity index	1.05746	0.0648255

3.3.2.2. VHSE

The VHSE scale is used to express the hydrophobic, steric and electronic properties of amino acids and polypeptides and has been used in QSAR studies of bitter peptides, the transporter associated with antigen processing (TAP) binding peptides, and oxytocin peptides (Y. W. Li & Li, 2013; Pan et al., 2012; J. B. Tong et al., 2015). Coincidentally, the VHSE scale was able to describe the properties of the amino acids in all three positions. As we see previously in the FASGAI model, Position 1 is the most important position in the VHSE model as well. It accounts for 5 of the 8 VIPs as seen in Table 4 and the components of the scale which include hydrophobic and electronic properties were described for n1 except its steric property. The variable n1V1 described the hydrophobic property of position 1 as positively correlating with the *Y* variable, suggesting that a hydrophobic amino acid at this position increases the inhibitory activity of the tripeptide. Out of the 5 variables for n1, 4 described its electronic properties; all except n1V8 signified that the property is negatively correlated with Y, this same trend was observed for amino acids at n3. This

could confirm the initial argument from the FASGAI model that nonpolar amino acids are important at the N- and C-terminus for increased potency.

The second position, n2 was further described by two variables n2V5 and n2V6 for the electronic properties of the amino acids. Based on the PLS regression coefficients, we see that the electronic properties of amino acid residues at position 2 are negatively correlated with inhibitory activity. As a result, amino acids which do not ionize easily and are uncharged are favorable at this position and we see this in peptides WKW, WQW, WRW, FKW and YHW which have ≤ 40% inhibitory activities. However, this contradicts the strong inhibitory activity of WEY which had the highest activity of 70% and has E in its second position.

Table 3.4. Summary of important peptide properties and their positions after PLS analysis using the VHSE model.

Variable	Position	Properties	VIP value	Regression Coefficient
n2V5	2	Electronic 1	1.51258	-0.49098
n2V6	2	Electronic 2	1.39158	-1.37393
n1V6	1	Electronic 2	1.31921	-0.146725
n1V5	1	Electronic 1	1.24206	-0.454247
n1V1	1	Hydrophobic 1	1.16734	0.215409
n3V5	3	Electronic 1	1.1095	-0.393183
n1V8	1	Electronic 4	1.08495	0.138649
n1V7	1	Electronic 3	1.0681	-0.361986

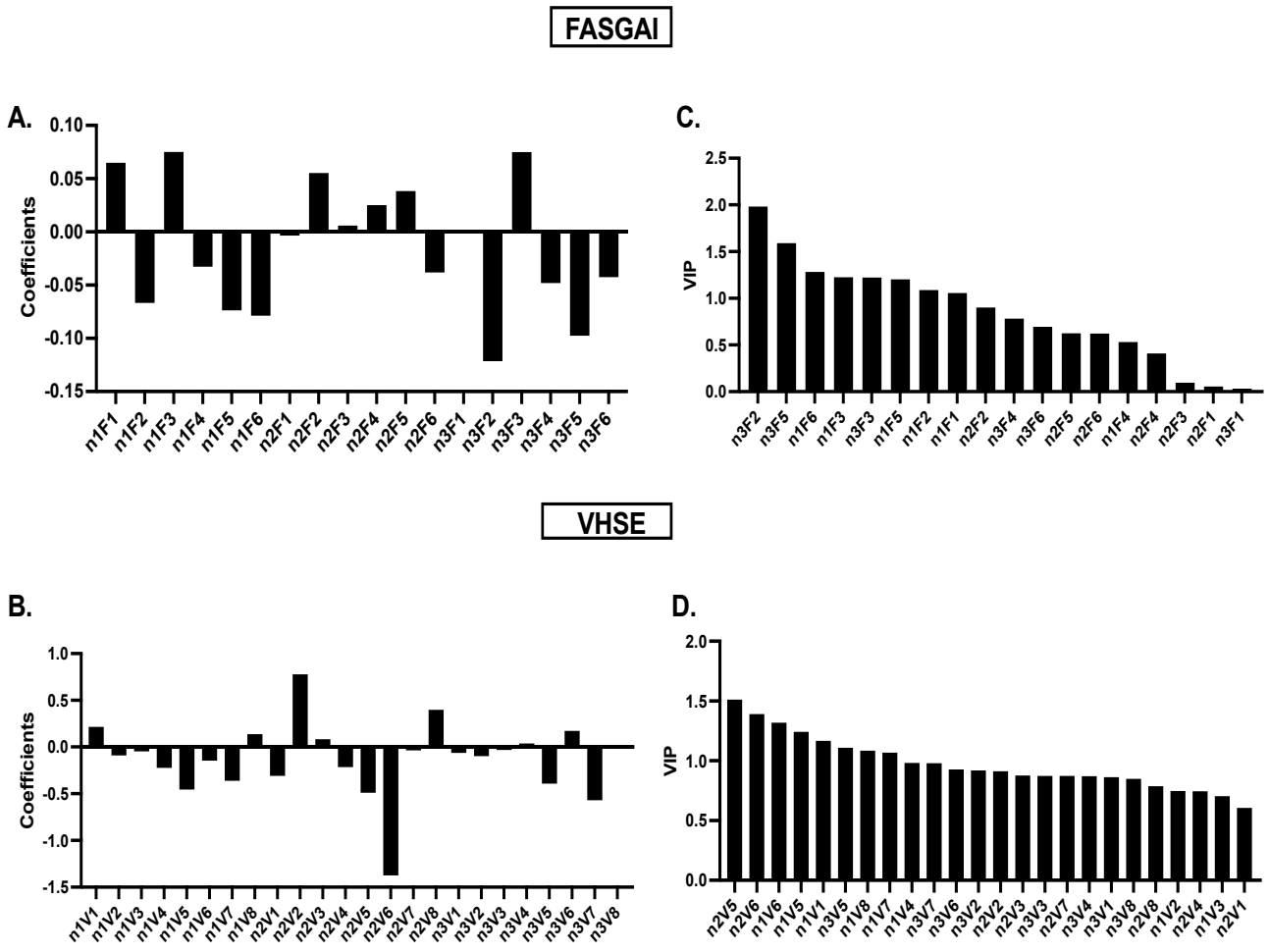

Figure 3.1. The VIP plot for sEH inhibitory tripeptide models of (A) FASGAI, and (B) VHSE, ales as well as their regression coefficients plots (C)FASGAI and (D) VHSE.

3.3.3. Inhibitory activity of the peptides

In order to identify and contribute to the already established list of 30 tripeptides with inhibitory activity for soluble epoxide hydrolase by Dang et al. (Dang et al., 2022), we screened 9 random tripeptides: QCV, QVC, CQV, QCA, VRS, VSS, LSQ, HIS and DIK. The soluble epoxide hydrolase converts its substrate PHOME into 6M2N, a fluorescent product that is monitored to determine the rate of the reaction. Successful inhibition of the enzyme will result in a lesser amount of 6M2N that can be observed in a reaction, indicated by a decrease in the relative fluorescence intensity. However, an increase in fluorescence intensity compared to the control sample group indicates an increase in the activity of sEH, enhanced by the added peptide.

Our study shows that at 100 μM, tripeptides; VRS, VSS, HIS, and DIK inhibited sEH significantly by 6.32 ± 0.97, 6.22 ± 1.02, 5.65 ± 0.55, and 8.65 ± 1.12 μM respectively. Whereas QCV, QVC, CQV, QCA and LSQ showed no inhibitory activities.

The activities observed not remotely close to the predicted activity from the stable model (FASGAI). While the FASGAI model predicted inhibitory activities between approximately 23-33% for the test set of peptides, the *in vitro* experiments showed that most of the peptides either did not have any inhibitory activity or had activities below 10% at 100μM concentration which is the same concentration of peptides used for the training set. This discrepancy in results could have resulted from various reasons including (i) half of the peptides from the test set (QCV, QVC, CQV) are highly hydrophilic, predominantly containing amino acids with polar side chains like Q, C at n1 and n3. These peptides showed negative inhibition suggesting that they helped promote the activity of sEH in the reaction, (ii) we see a bit of positive inhibition at 1% from QCA with the addition of A, a nonpolar amino acid at n3. Although this inhibition can be classified as next to nothing, the absence of an additional alkyl group on the side chain of A makes it less bulky than V which is a property of AAs at n3, (iii) the peptides VRS and VSS showed had improved inhibitory activities primarily because they contain V, which is the most hydrophobic and nonpolar amino acid at position n1, (iv) the peptide LSQ was able to inhibit up to 0.3% of the enzyme activity and we can attribute this low inhibitory activity to the net hydrophilicity of the peptide, (v) DIK, had the highest inhibitory activity of about 8.7%, D is a negatively charged AA and K is a positively charged AA suggesting that the elect

Overall, we see no similarity in the pattern of inhibition of the predicted vs observed. This is largely attributed to the low Q^2 value of the model, showing that the model has very low predictive capability.

3.4. Conclusion

In conclusion, this is the first QSAR investigation that uses 2D and 3D amino acid descriptors to elucidate the structural requirements for soluble epoxide hydrolase inhibition by dietary protein-derived peptides. We used FASGAI and VHSE scales to generate PLS regression models which show the hydrophobic and electronic properties of the tripeptide as the most important factors for increased sEH inhibitory activity. This led us to conclude that the presence of hydrophobic, nonpolar, bulky amino acid residues at the N-terminus (in order of preference; W >Y> F> I>L>V) and a bulky amino acid at the C-terminus (such as W, Y, F) contribute to the effectiveness of sEH-inhibiting tripeptides.

The insights drawn from the data are arguably non-generalizable because of the limited and nondiverse dataset which was used in this study. Therefore, there is a need to carry out more experimental investigations on more structurally diverse sEH inhibitory tripeptides in order to expand the available dataset, enabling the generation of improved models with satisfactory performances which can then be used in the prediction of the potency of tripeptides in sEH inhibition before they are synthesized for further analysis. Future investigations should also employ other peptide descriptors as well as molecular dynamics simulations which will shed more light on the behaviours of the amino acids in tripeptide sequence to obtain maximum inhibition of sEH activity.

3.5. References

Asen, N. D., Okagu, O. D., Udenigwe, C. C., & Aluko, R. E. (2022). In vitro inhibition of acetylcholinesterase activity by yellow field pea (Pisum sativum) protein-derived peptides as revealed by kinetics and molecular docking. *Frontiers in Nutrition*, *9*. https://doi.org/10.3389/fnut.2022.1021893

Beck, D. A. C., Alonso, D. O. V, Inoyama, D., & Daggett, V. (2008). *The intrinsic conformational propensities of the 20 naturally occurring amino acids and reflection of these propensities in proteins*. www.pnas.org/cgi/content/full/

Bhalla, J., Storchan, G. B., MacCarthy, C. M., Uversky, V. N., & Tcherkasskaya, O. (2006). Local flexibility in molecular function paradigm. *Molecular and Cellular Proteomics*, *5*(7). https://doi.org/10.1074/mcp.M500315-MCP200

Chakrabarti, S., Guha, S., & Majumder, K. (n.d.). *Food-Derived Bioactive Peptides in Human Health: Challenges and Opportunities*. https://doi.org/10.3390/nu10111738

Chen, D., Whitcomb, R., MacIntyre, E., Tran, V., Do, Z. N., Sabry, J., Patel, D. V., Anandan, S. K., Gless, R., & Webb, H. K. (2012). Pharmacokinetics and pharmacodynamics of AR9281, an inhibitor of soluble epoxide hydrolase, in single- and multiple-dose studies in healthy human subjects. *Journal of Clinical Pharmacology*, *52*(3). https://doi.org/10.1177/0091270010397049

Clark, J. J., Benson, M. L., Smith, R. D., & Carlson, H. A. (2019). Inherent versus induced protein flexibility: Comparisons within and between apo and holo structures. *PLoS Computational Biology*, *15*(1). https://doi.org/10.1371/journal.pcbi.1006705

Collantes, E. R., & Dunn, W. J. (1995). Amino Acid Side Chain Descriptors for Quantitative Structure-Activity Relationship Studies of Peptide Analogues. *Journal of Medicinal Chemistry*, *38*(14). https://doi.org/10.1021/jm00014a022

Daliri, E. B. M., Oh, D. H., & Lee, B. H. (2017). Bioactive peptides. In *Foods* (Vol. 6, Issue 5, pp. 1–21). MDPI AG. https://doi.org/10.3390/foods6050032

Dang, J., Du, S., & Wang, L. (2022). Screening and Identification of Novel Soluble Epoxide Hydrolase Inhibitors from Corn Gluten Peptides [Article]. *Foods*, *11*(22), 3695. https://doi.org/10.3390/foods11223695

Ganguly, A., Sharma, K., & Majumder, K. (2021). Methodologies for studying the structure-function relationship of food-derived peptides with biological activities. In *Biologically Active Peptides: From Basic Science to Applications for Human Health*. https://doi.org/10.1016/B978-0-12-821389-6.00008-X

Gu, Y., Majumder, K., & Wu, J. (2011). QSAR-aided in silico approach in evaluation of food proteins as precursors of ACE inhibitory peptides. *Food Research International*, *44*(8). https://doi.org/10.1016/j.foodres.2011.01.051

Guedes, A., Galuppo, L., Hood, D., Hwang, S. H., Morisseau, C., & Hammock, B. D. (2017). Soluble epoxide hydrolase activity and pharmacologic inhibition in horses with chronic severe laminitis. *Equine Veterinary Journal*, *49*(3). https://doi.org/10.1111/evj.12603

Hammock, B. D., McReynolds, C. B., Wagner, K., Buckpitt, A., Cortes-Puch, I., Croston, G., Lee, K. S. S., Yang, J., Schmidt, W. K., & Hwang, S. H. (2021). Movement to the Clinic of Soluble Epoxide Hydrolase Inhibitor EC5026 as an Analgesic for Neuropathic Pain and for Use as a Nonaddictive Opioid Alternative. *Journal of Medicinal Chemistry*, *64*(4). https://doi.org/10.1021/acs.jmedchem.0c01886

Hellberg, S., Sjöström, M., Skagerberg, B., & Wold, S. (1987). Peptide Quantitative Structure-Activity Relationships, a Multivariate Approach. *Journal of Medicinal Chemistry*, *30*(7). https://doi.org/10.1021/jm00390a003

Inceoglu, B., Bettaieb, A., Trindade Da Silva, C. A., Lee, K. S. S., Haj, F. G., & Hammock, B. D. (2015). Endoplasmic reticulum stress in the peripheral nervous system is a significant driver of neuropathic pain. In *Proceedings of the National Academy of Sciences of the United States of America* (Vol. 112, Issue 29). https://doi.org/10.1073/pnas.1510137112

Kidera, A., Konishi, Y., Oka, M., Ooi, T., & Scheraga, H. A. (1985). Statistical analysis of the physical properties of the 20 naturally occurring amino acids. *Journal of Protein Chemistry*, *4*(1). https://doi.org/10.1007/BF01025492

Lazaar, A. L., Yang, L., Boardley, R. L., Goyal, N. S., Robertson, J., Baldwin, S. J., Newby, D. E., Wilkinson, I. B., Tal-Singer, R., Mayer, R. J., & Cheriyan, J. (2016). Pharmacokinetics, pharmacodynamics and adverse event profile of GSK2256294, a novel soluble epoxide hydrolase inhibitor. *British Journal of Clinical Pharmacology*, *81*(5). https://doi.org/10.1111/bcp.12855

Li, Y. W., & Li, B. (2013). Characterization of structure-antioxidant activity relationship of peptides in free radical systems using QSAR models: Key sequence positions and their amino acid properties. *Journal of Theoretical Biology*, *318*. https://doi.org/10.1016/j.jtbi.2012.10.029

Li, Z. L., Li, G. R., Shu, M., Sun, J. Y., Yang, S. Bin, Mei, H., Zhang, M. J., Zhou, P., Wu, S. R., Chen, G. H., Lu, F. L., & Lu, T. T. (2008). A novel vector of topological and structural information for amino acids and its QSAR applications for peptides and analogues. *Science in China, Series B: Chemistry*, *51*(10). https://doi.org/10.1007/s11426-008-0040-5

Liang, G., & Li, Z. (2007). Factor analysis scale of generalized amino acid information as the source of a new set of descriptors for elucidating the structure and activity relationships of cationic antimicrobial peptides. *QSAR and Combinatorial Science*, *26*(6). https://doi.org/10.1002/qsar.200630145

Liang, G., Yang, L., Chen, Z., Mei, H., Shu, M., & Li, Z. (2009). A set of new amino acid descriptors applied in prediction of MHC class I binding peptides. *European Journal of Medicinal Chemistry*, *44*(3). https://doi.org/10.1016/j.ejmech.2008.06.011

Liang, G., Yang, L., Kang, L., Mei, H., & Li, Z. (2009). Using multidimensional patterns of amino acid attributes for QSAR analysis of peptides. *Amino Acids*, *37*(4). https://doi.org/10.1007/s00726-008-0177-8

Liang, G. Z., Shu, M., & Li, S. S. Z. L. (2008). A new set of amino acid descriptors for the development of quantitative sequence-activity modelings of HLA-A*0201 restrictive CTL epitopes. *Journal of the Chinese Chemical Society*, *55*(5). https://doi.org/10.1002/jccs.200800174

Luo, J., Hu, S., Fu, M., Luo, L., Li, Y., Li, W., Cai, Y., Dong, R., Yang, Y., Tu, L., & Xu, X. (2021). Inhibition of soluble epoxide hydrolase alleviates insulin resistance and hypertension via downregulation of SGLT2 in the mouse kidney. *Journal of Biological Chemistry*, *296*. https://doi.org/10.1016/j.jbc.2021.100667

Mei, H., Zhou, Y., Sun, L. L., & Li, Z. L. (2004). A new descriptor of amino acids and its application in peptide QSAR. *Acta Physico - Chimica Sinica*, *20*(8). https://doi.org/10.3866/pku.whxb20040808

Mollica, A., Zengin, G., Durdagi, S., Ekhteiari Salmas, R., Macedonio, G., Stefanucci, A., Dimmito, M. P., & Novellino, E. (2019). Combinatorial peptide library screening for discovery of diverse α-glucosidase inhibitors using molecular dynamics simulations and binary QSAR models. *Journal of Biomolecular Structure and Dynamics*, *37*(3). https://doi.org/10.1080/07391102.2018.1439403

Nakagawa, Y., Wheelock, C. E., Morisseau, C., Goodrow, M. H., Hammock, B. G., & Hammock, B. D. (2000). 3-D QSAR analysis of inhibition of murine soluble epoxide hydrolase (MsEH) by benzoylureas, arylureas, and their analogues. *Bioorganic and Medicinal Chemistry*, *8*(11). https://doi.org/10.1016/S0968-0896(00)00198-X

Nazari, M., Rezaee, E., & Tabatabai, S. A. (2022). A Comprehensive Review of Soluble Epoxide Hyådrolase Inhibitors Evaluating their Structure-Activity Relationship. *Mini-Reviews in Medicinal Chemistry*, *23*(1). https://doi.org/10.2174/1389557522666220531152812

Obeme-Nmom, J.I., Abioye, R.O., Fatoki, T.H., & Udenigwe, C.C. (2023). Biomolecular Interactions and Inhibition Kinetics of Human Soluble Epoxide Hydrolase by Tetrapeptide YMSV. *Journal of Food Bioactives*, *21*. https://doi.org/10.31665/jfb.2023.18341

Pan, X. C., Mei, H., Xie, J. A., Lü, J., Wang, Q., Zhang, Y. L., & Tan, W. (2012). Prediction of TAP binding affinity of peptide and selection specificity using VHSE descriptors. *Gaodeng Xuexiao Huaxue Xuebao/Chemical Journal of Chinese Universities*, *33*(11). https://doi.org/10.7503/cjcu20120056

Pathak, S., Mishra, A., Sonawane, G., Sonawane, K., Rawat, S., Raizaday, A., Singh, S. K., & Gupta, G. (2023). In silico pharmacology. In *Computational Approaches in Drug Discovery, Development and Systems Pharmacology*. https://doi.org/10.1016/B978-0-323-99137-7.00006-X

Rose, T. E., Morisseau, C., Liu, J. Y., Inceoglu, B., Jones, P. D., Sanborn, J. R., & Hammock, B. D. (2010). 1-Aryl-3-(1-acylpiperidin-4-yl)urea inhibitors of human and murine soluble epoxide hydrolase: Structure-activity relationships, pharmacokinetics, and reduction of inflammatory pain. *Journal of Medicinal Chemistry*, *53*(19). https://doi.org/10.1021/jm100691c

Shu, M., Mei, H., Yang, S., Liao, L., & Li, Z. (2009). Structural parameter characterization and bioactivity simulation based on peptide sequence. *QSAR and Combinatorial Science*, *28*(1). https://doi.org/10.1002/qsar.200710169

Singh, N., Barnych, B., Morisseau, C., Wagner, K. M., Wan, D., Takeshita, A., Pham, H., Xu, T., Dandekar, A., Liu, J. Y., & Hammock, B. D. (2020). N-Benzyl-linoleamide, a Constituent of Lepidium meyenii (Maca), Is an Orally Bioavailable Soluble Epoxide Hydrolase Inhibitor That Alleviates Inflammatory Pain. *Journal of Natural Products*, *83*(12). https://doi.org/10.1021/acs.jnatprod.0c00938

Smith, D. K., Radivojac, P., Obradovic, Z., Dunker, A. K., & Zhu, G. (2003). Improved amino acid flexibility parameters. *Protein Science*, *12*(5). https://doi.org/10.1110/ps.0236203

Sneath, P. H. A. (1966). Relations between chemical structure and biological activity in peptides. *Journal of Theoretical Biology*, *12*(2). https://doi.org/10.1016/0022-5193(66)90112-3

Sun, C.-P., Zhang, X.-Y., Morisseau, C., Hwang, S. H., Zhang, Z.-J., Hammock, B. D., & Ma, X.-C. (2021). Discovery of Soluble Epoxide Hydrolase Inhibitors from Chemical Synthesis and Natural Products [Article]. *Journal of Medicinal Chemistry*, *64*(1), 184–215. https://doi.org/10.1021/acs.jmedchem.0c01507

Tian, F., Yang, L., Lv, F., Yang, Q., & Zhou, P. (2009). In silico quantitative prediction of peptides binding affinity to human MHC molecule: An intuitive quantitative structure-activity relationship approach. *Amino Acids*, *36*(3). https://doi.org/10.1007/s00726-008-0116-8

Tian, F., Zhou, P., & Li, Z. (2007). T-scale as a novel vector of topological descriptors for amino acids and its application in QSARs of peptides. *Journal of Molecular Structure*, *830*(1–3). https://doi.org/10.1016/j.molstruc.2006.07.004

Tong, J. B., Chang, J., Liu, S. L., & Bai, M. (2015). A quantitative structure-activity relationship (QSAR) study of peptide drugs based on a new of amino acids. *Journal of the Serbian Chemical Society*, *80*(3). https://doi.org/10.2298/JSC140604069T

Tong, J., Liu, S., Zhou, P., Wu, B., & Li, Z. (2008). A novel descriptor of amino acids and its application in peptide QSAR. *Journal of Theoretical Biology*, *253*(1). https://doi.org/10.1016/j.jtbi.2008.02.030

Udenigwe, C. C., Li, H., & Aluko, R. E. (2012). Quantitative structure-activity relationship modeling of renin-inhibiting dipeptides. *Amino Acids*, *42*(4). https://doi.org/10.1007/s00726-011-0833-2

Vázquez, J., Ginex, T., Herrero, A., Morisseau, C., Hammock, B. D., & Luque, F. J. (2023). Screening and Biological Evaluation of Soluble Epoxide Hydrolase Inhibitors: Assessing the Role of Hydrophobicity in the Pharmacophore-Guided Search of Novel Hits. *Journal of Chemical Information and Modeling*. https://doi.org/10.1021/acs.jcim.3c00301

Wagner, K. M., McReynolds, C. B., Schmidt, W. K., & Hammock, B. D. (2017). Soluble epoxide hydrolase as a therapeutic target for pain, inflammatory and neurodegenerative diseases. *Pharmacology & Therapeutics*, *180*, 62–76. https://doi.org/10.1016/J.PHARMTHERA.2017.06.006

Yang, L., Shu, M., Ma, K., Mei, H., Jiang, Y., & Li, Z. (2010). ST-scale as a novel amino acid descriptor and its application in QSAM of peptides and analogues. *Amino Acids*, *38*(3). https://doi.org/10.1007/s00726-009-0287-y

CHAPTER 4 – CONCLUSION

The biological activities of food-derived peptides have gained more engagement over the last decade with interest in discovering more ways these peptides can be used in nutrition to preserve human health. However, our knowledge of the manner in which dietary peptides and the targets for severe depressive disease interplay is still quite limited at this point. Therefore, the aim of this study was to explore the chances of food-based peptides having anti-depressive actions by studying their effects on the enzymatic activities of human sEH, a recently identified target for depression. This helped to determine whether or not food-based peptides have anti-depressant properties. Moreover, short-chain food peptides can escape gastrointestinal digestion into the liver-brain axis where soluble epoxide hydrolase is largely active.

According to our findings by enzyme kinetics and molecular docking, YMSV is a novel mixed-competitive inhibitor of sEH that exerts its inhibitory activity through hydrogen bonding with both active and non-active site residues of sEH. The proportions of the enzyme's alpha helices, beta sheets, and disordered random coils are all altered by YMSV inhibition. In addition, the quantitative-structure activity relationship study demonstrated that the structural properties of peptides promote their inhibitory potency for the soluble epoxide hydrolase enzyme, especially their hydrophobic property. However, the study could not generate a good/ strong model for the prediction of the inhibitory activity of peptides due to a limited training list of peptides.

Subsequent investigations should encompass the advancement of processing techniques aimed at liberating more bioactive peptides from their precursor proteins, alongside evaluations of their *in vivo* physiological bioactivity and pharmacokinetics. there is a need for the evaluation of more peptides in order to expand the test list to generate a strong model. It is suggested that cell culture analysis using liver and brain cells from depressive animal models can be done to expand the knowledge of peptide inhibition of sEH. Likewise, animal studies should be designed where food-peptide sEH inhibitors can be administered orally or intravenously to the subject for a period after which inflammatory biomarkers would be measured to check for anti-inflammatory and anti-depressive activities. Peptidomics and advanced bioinformatics may also be employed to facilitate the discovery of a wide range of important food peptide motifs that can be further investigated as sEH inhibitors. The implementation of these will help with the development of functional meals for those suffering from mild or severe depression.